(Table XI), making it difficult to comment further.

The conformation of **4** contrasts with that of **3** as well as the hydrocarbon analogue, cyclotetracosane, which adopts a compact [3939] quadrangular conformation.[60,61] This difference may be attributable to the preference for gauche torsion angles about Se–C bonds. It is thus noteworthy that every Se–C bond has a gauche C–Se–C–C torsion angle.

The CP-MAS ^{77}Se NMR spectrum of **4** shows only three resonances of equal intensity, consistent with the presence of a single conformer having crystallographic inversion symmetry. Also consistent is the CP-MAS ^{13}C NMR spectrum, which shows five resolved resonances in a ratio of 2:3:1:1:2, accounting for the nine unique carbon sites in the asymmetric unit.

The placement of the selenium atoms in corner positions of **5** confirms the preference for the gauche torsion angles to occur about Se–C bonds. Of the structures reported here this is the only one to conform to the "diamond lattice" formalism.

The CP-MAS ^{77}Se NMR spectrum of **5** shows two peaks, as expected because of the crystallographic center of inversion. The CP-MAS ^{13}C NMR spectrum shows four resolved resonances in the ratio of 1:1:2:1, consistent with the presence of five unique carbon sites in the molecule.

The potential ability of coronands **3**, **4**, and **5** to serve as complexing agents for soft metal ions is currently under investigation, compounds **1a**, **1b**, **2a**, and **2b** being considered as less likely candidates owing to restrictions imposed by the connectivities in the latter derivatives. In this regard, several complexes of **3** and **4** with Cu(I), Cu(II), Ag(I), and Pd(II) ions have been prepared.[62]

Conclusions

All the structures display a preference for gauche torsion angles about the Se–C bonds. The crystal structure of **2a** as well as the solution conformation of **1a** and **1b** show, in addition, a bias toward gauche torsion angles about the bonds to the "anomeric" carbon atoms. The crystal structures of **1a** and **3** show that these preferences can be overridden by other effects such as crystal packing and the tendency of the larger rings to adopt compact conformations (rather than more open, ideally unstrained conformations). The largest rings **2a** and **4** display compact conformations that feature sequences of gauche torsion angles of the same sign, in contrast to the large, even-membered cycloalkanes, which feature two long parallel sides composed of sequences of anti torsion angles.

Acknowledgment. We thank the Natural Sciences and Engineering Research Council of Canada for financial support.

Supplementary Material Available: Table of experimental details for the X-ray structural analysis of **3**, table of atomic coordinates and isotropic or equivalent isotropic thermal parameters for **3**, tables of hydrogen atom coordinates and isotropic thermal parameters for **1a**, **2a**, **4**, and **5**, tables of anisotropic thermal parameters for Se and C atoms of **1a**, **2a**, **4**, and **5**, table of anisotropic thermal parameters for Se atoms of **3**, tables of bond distances, bond angles, and torsion angles for **3** (22 pages); tables of observed and calculated structure factors for **1a**, **2a**, **3**, **4**, and **5** (67 pages). Ordering information is given on any current masthead page.

(60) Groth, P. *Acta Chem. Scand.* **1979**, *A33*, 199.
(61) Ando, I.; Yamanobe, T.; Sorita, T.; Komoto, T.; Sato, H.; Deguchi, K.; Imanari, M. *Macromolecules* **1984**, *17*, 1955. Yamanobe, T.; Sorita, S.; Ando, I.; Sato, H. *Makromol. Chem.* **1985**, *186*, 2071.
(62) Gu, J.-H.; Pinto, B. M., unpublished results.

Properties and Reactivity of Metallocarboxylates. Characterization of Aquobis(ethylenediamine)(hydroxycarbonyl)cobalt(III) $[(H_2O)(en)_2Co(C(O)OH)]^{2+}$ and Its Ethyl Ester, *trans*-$[Co(en)_2(CF_3CO_2)(C(O)OC_2H_5)]PF_6$

Nêstor E. Katz,[1] David J. Szalda,[2] Mei H. Chou, Carol Creutz,* and Norman Sutin

Contribution from the Department of Chemistry, Brookhaven National Laboratory, Upton, New York 11973. *Received October 31, 1988*

Abstract: The title metallocarboxylate, first described by Vaudo et al. (*J. Am. Chem. Soc.* **1972**, *94*, 6655) has been further investigated, and its ethyl ester, prepared. Crystals of the ester (ethoxycarbonyl) $[Co(NH_2CH_2CH_2NH_2)_2(O_2CCF_3)(C(O)OC_2H_5)]PF_6$ are monoclinic: space group $P2_1/c$ with $a = 9.077$ (1) Å, $b = 16.375$ (2) Å, $c = 12.919$ (2) Å, $\beta = 92.15$ (1)°, $V = 1918.9$ (7) Å^3, $Z = 4$, and refined to a final R value of 0.079. The ethylenediamine ligands are trans to one another (Co–N ave, 1.944 (13) Å) with axial ligands $CF_3CO_2^-$ (Co–O, 2.046 (7) Å) and $-C(O)OC_2H_5^-$ (Co–C, 1.922 (9) Å; C=O 1.196 (9) Å, $\nu_{C=O}$ 1645 cm^{-1}). The aquo hydroxycarbonyl complex (UV–vis: λ_{max}, nm [ϵ, M^{-1} cm^{-1}] 410 [125], 314 sh [580], 262 [5200]) is a dibasic acid with $pK_1 = 2.5 \pm 0.5$ and $pK_2 = 3.7 \pm 0.5$ at 15 °C and 0.5 M ionic strength and, at pH > 5, is present as the neutral hydroxy-oxycarbonyl complex $Co(en)_2(OH)(CO_2)$ (UV–vis: 450 [100], 357 [245], 318 [280], 266 [9000]). The aquo ethoxycarbonyl complex (UV–vis: 424 [113], 320 sh [210], 264 [5100]) is a monobasic acid with $pK_a = 8.7 \pm 0.2$ at 25 °C and 0.5 M ionic strength and, at high pH, is converted to $Co(en)_2(OH)(CO_2Et)^+$ (UV–vis: 430 [159], 329 sh [260]). The ethoxy function is hydrolyzed very slowly in the latter complexes (pH, k_{obsd}: 1, 2.5×10^{-6} s^{-1}; 7, $< 2 \times 10^{-7}$ s^{-1}; 13, 3×10^{-6} s^{-1}) to yield ethanol and the hydroxy- or oxycarbonyl, depending upon the pH. At pH > 0 the oxy- or hydroxycarbonyl complex undergoes decomposition through the singly protonated $Co(en)_2(H_2O)(CO_2)^+$, exhibiting a rate maximum ($k_{obsd} \approx 3 \times 10^{-3}$ s^{-1}, 25 °C) at ca. pH 3.2.

Metallocarboxylate (oxycarbonyl) complexes play an important role in diverse reactions of catalytic importance:[3] Under water–gas shift conditions,[4] they may be formed by nucleophilic attack of hydroxide ion on a metal carbonyl. In this context, the rate and

0002-7863/89/1511-6591$01.50/0

mechanism of reductive elimination of CO_2 from M–CO_2 is of considerable interest and importance. In some systems this step is rate limiting and determines the catalytic efficiency of the system. Metallocarboxylate complexes are also of importance in the area of carbon dioxide fixation and reduction[5] as they may be formed through the reaction of a low-valent (often d^8) metal center with CO_2. Here, both reversible CO_2 binding and binding leading to reduction (generally to CO or formate ion) have been observed. In this context, the factors determining the affinity of the metal center for CO_2 and the factors determining the CO_2 reduction rates and products are of importance. Finally, the basic coordination chemistry of metallocarboxylate complexes is of considerable interest. While a number of organometallic species of this class are known, only a few reports of such fundamental properties as the pK_a of MC(O)OH, etc., have appeared. We were intrigued by an early report[6] of photochemically prepared Co(en)$_2$(H$_2$O)(CO$_2$H)$^{2+}$ (**1**), apparently the metallocarboxylic acid derivative of a classical coordination complex, and decided to further investigate its physical properties and chemical reactivity. In the course of our studies we inadvertently prepared a derivative, its ethyl ester, **2**. The properties of both, as well as an X-ray structural determination of the ester derivative, are reported here.

Experimental Section

Preparations. [Co(en)$_2$(CF$_3$CO$_2$)(C(O)OC$_2$H$_5$)]PF$_6$. A modification of the procedure of Vaudo et al.[6b] was used to generate the carboxylate complex photochemically. Here CF_3CO_2H was chosen as eluant because of its volatility, and the original Dowex resin has been replaced with Sephadex. A solution of 0.5 g of [(en)$_2$Co(C$_2$O$_4$)]Cl·H$_2$O (1.56 mmol)[7] in 100 mL of 0.1 M HCl was photolyzed under Ar for 5 min using a medium-pressure Hg (Hanovia, immersion) lamp. The solution was then chromatographed at 5 °C on a water-jacketed Sephadex SP-C25 column (3 × 12 cm). The unreacted oxalate complex (~20%) was eluted with 0.2 M CF_3CO_2H, while the yellow carboxylate (2+) complex was eluted with 0.3 M CF_3CO_2H. (The central (pink) Co_{aq}^{2+} fraction was discarded.) The yellow fraction (λ_{max} 422 nm) was collected in an ice bath and "freeze-dried" on a rotary evaporator. The resulting orange oil or solid was mixed with 2 mL of ethanol and 8 mL of diethyl ether and stored at −10 °C overnight. The orange solution was separated by filtration from the white solid, enH$_2$(CF$_3$CO$_2$)$_2$ (identified by IR; yield 27%), that formed. To the filtrate was added 6 mL of ethanol containing 0.5 g of NH_4PF_6 (filtered prior to addition); the solution volume was reduced ~50% by evaporation under vacuum, and the flask was stored at −10 °C for ~3 days. The yellow microcrystalline solid obtained was collected on a filter, washed with cold ethanol and ether, and dried in air. Yield: 34.5 mg (4.3% based on Co(en)$_2$(C$_2$O$_4$)$^+$). Anal. Calcd for [(en)$_2$Co(C(O)OC$_2$H$_5$)(CO$_2$CF$_3$)]PF$_6$: C, 21.1; H, 4.5; N, 11.0; Co, 11.5; PF_6^-, 28; $CF_3CO_2^-$, 22. Found: C, 20.9; H, 3.6; N, 10.9; Co, 11.0; PF_6^-, 27; $CF_3CO_2^-$, 21.

The crystals used for the X-ray diffraction studies were grown from water: 10 mg was dissolved in 1 mL of water, and the solution was filtered and evaporated slowly under vacuum in a bell jar.

A solid sample of [(en)$_2$Co(OH$_2$)(CO$_2$Et)](PF$_6$)$_2$ was obtained as follows: The $CF_3CO_2^-$-containing material above was dissolved in water and passed through a Sephadex A-25 column in the PF_6^- form, and the solution was then evaporated to dryness.

Method A. Co(en)$_2$(H$_2$O)(CO$_2$H)$^{2+}$. The above photolysis and chromatography procedure was followed with $HClO_4$/$LiClO_4$ as eluant instead of CF_3CO_2H. The Co(en)$_2$(H$_2$O)(CO$_2$H)$^{2+}$ was eluted with 0.1 M $HClO_4$/0.2 M $LiClO_4$ and stored under Ar at −10 °C.

Method B. Co(en)$_2$(OH)(CO$_2$). Rather late in the course of this study we recognized that Co(en)$_2$(H$_2$O)(CO$_2$H)$^{2+}$ is a dibasic acid. This suggested an alternative to the cation-exchange chromatography in acid (Method A, which does not separate Co(en)$_2$(H$_2$O)(CO$_2$H)$^{2+}$ from enH$_2^{2+}$). The Co(en)$_2$(C$_2$O$_4$)$^+$ photolysis was carried out as described above but in 0.05 M HCl. The photolyzed solution was transferred to an Ar-blanketed flask, and 6.5 mL of 0.5 M Na_3PO_4 was added to give a final pH ≥ 7, under which conditions the desired material is expected to be a neutral species. The solution was loaded onto a Sephadex SP-C5 column in the Na^+ form (preliminary experiment) or onto an AG50W2X column (25 mL, 1.6-cm diameter) in the Na^+ form under argon. The column was washed with ~200 mL of 0.01 M pH 7 phosphate buffer; then the desired orange carboxylate was eluted in 0.03 M phosphate/0.06 M $NaClO_4$ and collected under argon in an ice bath, with the pink parent Co(en)$_2$(C$_2$O$_4$)$^+$ remaining on the column; Co^{2+} formed in the photolysis settled at the top of the column as a violet phosphate precipitate. Cold alkaline solutions of Co(en)$_2$(OH)(CO$_2$) are nearly indefinitely stable (>1 mo) in the absence of oxygen. (Yield: ~10%; ~150 mL of 1 × 10^{-3} M Co(en)$_2$(OH)(CO$_2$)). The total cobalt and cobalt(II) concentrations of the solution were determined, and the CO_2 content was analyzed: To 2.5 mL stock solution, bubbled with Ar for 15 min at room temperature was added 0.5 mL of 0.5 M Ce(IV) in 2.5 M H_2SO_4. The solution was mixed, left 30 min, and then analyzed for CO_2 by GC. Results: total [Co] = 1.05 × 10^{-3} M; [Co(II)] ≤ 3 × 10^{-5} M; ["CO_2"] = 1.0 × 10^{-3} M (all are averages of at least three determinations). Co(en)$_2$(OH)(CO$_2$) spectrum: λ_{max}, nm (ϵ_{max}, M^{-1} cm^{-1}) 450 (1.00 × 10^2), 357 (2.45 × 10^2), 318 (2.80 × 10^2) at pH 6–7 (ϵ values based on Co analyses above).

Kinetic runs were performed either (a) at 260 nm with (0.2–2) × 10^{-4} M Co(en)$_2$(CO$_2$)$_{aq}$ or (b) at 420–450 nm with 10 times more concentrated solutions. The runs were initiated by (a) injecting 0.5 mL of stock solution into 2.5 mL of buffered mixture in a 1-cm cell or (b) injecting a small volume of buffer (0.5 or 3.0 mL) into stock cobalt solution (2.5 or 15.0 mL) in a spectrophotometer cell (1 or 5 cm). **Buffers** and cobalt stock solutions were bubbled with Ar and brought to 25 °C prior to mixing. Transfers were carried out by syringe techniques. The spectrophotometer cell was sealed after injections by closing the septum-topped stopcock. The Co(en)$_2$(H$_2$O)(C(O)OEt)$^{2+}$ hydrolysis kinetics were carried out in the same way except that a weighed sample of the solid (instead of a stock solution) was used.

Analyses. Analyses for C, H, and N were performed by Schwarzkopf Microanalytical Laboratory, and Co (atomic absorption) and anion (ion chromatography) analyses were done by E. Norton. Co(II) was determined by the Kitson method.[8] Gases were analyzed by GC: N_2, CH_4, and CO (He carrier) and H_2 (Ar carrier) on molecular sieve (5A); CO_2 on Chromosorb (He carrier). Ethanol was determined on a Perkin-Elmer Sigma 3B FID gas chromatograph (Carbowax 20 M, 80 °C) with internal standard acetone (1 mM) and calibration against known aqueous ethanol solutions (0.1–2 mM): typical injection volume, 2 μL. Formaldehyde was analyzed with chromotropic acid:[9] 2.00 mL of solution (0.3–1.5) × 10^{-4} M in formaldehyde was transferred to a 50-mL volumetric flask containing 0.10 g of chromotropic acid (4,5-dihydroxynaphthalene-2,7-disulfonic acid; MCB), and 7.0 mL of 18 M H_2SO_4 was added cautiously. The flask was heated 30 min in a boiling water bath, cooled, and diluted to the mark with water. The cooled solution was transferred to a 10-cm cell, and the visible spectrum, measured against that of a reagent blank: ϵ_{eff} = 1.4 × 10^4 M^{-1} cm^{-1}. No interference by Co^{2+} or enH$_2^{2+}$ was found.

Instrumentation and Techniques. IR spectra of KBr pellets or Nujol mulls were measured using a Nicolet MX-1 FT-IR spectrophotometer. UV–visible spectra were obtained with HP 8451A, Cary 210, and Cary 17 spectrophotometers. pH measurements were carried out with a Metrohm 632 pH meter, calibrated with standard buffers. ^{1}H NMR spectra were recorded in CD_3CN, using a Bruker AM-300 FT-NMR spectrometer.

Collection and Reduction of X-ray Data. [Co(en)$_2$(O$_2$CCF$_3$)(CO$_2$Et)]PF$_6$ crystallizes as clusters of yellow crystals. Single crystals were cut from the clusters, coated with petroleum jelly, and mounted in a glass capillary. A crystal 0.10 × 0.20 × 0.85 mm with faces (1$\bar{1}\bar{1}$), ($\bar{1}$11), ($\bar{1}\bar{1}$1), (11$\bar{1}$), (001), and (00$\bar{1}$) was used in the X-ray study. The crystal exhibited monoclinic symmetry with systematic absences $h0l$, l = 2n + 1, and $0k0$, k = 2n + 1, consistent with the space group $P2_1/c$-C_{2h}^5 (No. 14).[10]

(1) On leave of absence from Facultad de Bioquímica, Química, y Farmacia, Universidad Nacional de Tucumán, Argentina. Member of the "Carrera del Investigador Científico", CONICET, Argentina.

(2) To whom questions concerning the X-ray crystallography should be addressed. Permanent address: Department of Natural Science, Baruch College, Manhattan, NY 10010.

(3) (a) Ford, P. C.; Rokicki, A. *Adv. Organomet. Chem.* **1988**, *28*, 137. (b) Halpern, J. *Comments Inorg. Chem.* **1981**, *1*, 3.

(4) See: Ford, P. C. *Acc. Chem. Res.* **1981**, *14*, 31 and references cited therein.

(5) See: *Catalytic Activation of Carbon Dioxide*; Ayers, W. M., Ed.; ACS Symposium Series No. *363*; American Chemical Society: Washington, DC, 1988. Behr, A., *Carbon Dioxide Activation by Metal Complexes*; VCH: New York, 1988; and references cited therein.

(6) (a) Vaudo, A. F.; Kantrowitz, E. R.; Hoffman, M. Z. *J. Am. Chem. Soc.* **1971**, *93*, 6698. (b) Vaudo, A. F.; Kantrowitz, E. R.; Hoffman, M. Z.; Papaconstantinou, E.; Endicott, J. F. *J. Am. Chem. Soc.* **1972**, *94*, 6655. (c) Kantrowitz, E. R.; Hoffman, M. Z.; Schilling, K. M. *J. Phys. Chem.* **1972**, *76*, 2492. (d) Kantrowitz, E. R. *J. Chem. Educ.* **1974**, *51*, 202.

(7) Jordan, N. T.; Froebe, L. R. *Inorg. Synth.* **1978**, *18*, 97.

(8) Kitson, R. E. *Anal. Chem.* **1950**, *22*, 664.

(9) Bricker, C. E.; Vail, W. A. *Anal. Chem.* **1950**, *22*, 720.

(10) *International Tables for X-ray Crystallography*, 3rd ed.; Kynoch Press: Birmingham, U.K., 1969; Vol. I, p 99.

Table I. Experimental Details of the X-ray Diffraction Study of $[Co(H_2NCH_2CH_2NH_2)_2(CO_2CH_2CH_3)(O_2CCF_3)]PF_6$

	(A) Crystal Parameters[a] at 23 °C
a, Å	9.077 (1)
b, Å	16.375 (2)
c, Å	12.919 (2)
β, deg	92.15 (1)
V	1918.9 (7)
Z	4
mol wt	510.2
space gp	$P2_1/c$
ρ(exptl), g cm^{-3}	1.76 (1)[b]
ρ(calc), g cm^{-3}	1.766
	(B) Measurement of Intensity Data
instrument	Enraf-Nonius Cad 4 diffractometer
radiatn	Cu Kα (λ = 1.540 51 Å), graphite monochromated
2θ limits	4–120°
scan type	θ (crystal)–2θ (counter)
std	three reflcns measd after each 1 h of exposure showed no systematic variatns
	(C) Treatment of Intensity Data[c]
reduction to preliminary F_o and $\sigma(F_o)$	corrn for bkgd, attenuators and Lorentz polarizn effects of monochromatized X-radiatn in the usual manner[c]
absptn corrn	μ = 87.3 cm^{-1}, max and min transmissn coeff 0.4822 and 0.07352, respectively
obsd data	of the 6341 reflcns collected, including systematic absences, the 5031 obsd reflcns have merged into 2640 unique reflcns (R_{ave} = 0.056) with 1842 reflcns with $F_o \geq 3\sigma(F_o)$ used for the refinement

[a] From the least-squares fit to the setting angles of 25 reflections with $2\theta > 40°$. [b] Neutral bouyancy method using chloroform and bromoform. [c] See: Szalda, D. J.; Keene, F. R. *Inorg. Chem.* **1986**, *25* 2795.

Crystal data and details of data collection and reduction are given in Table I.

Determination and Refinement of Structure. The coordinates for the cobalt atom were determined from a Patterson map,[11] and the remaining atoms were located by a series of difference Fourier maps. Four of the six fluorine atoms of the PF_6^- anions were found to be disordered. A model with two sets of fluorine atoms, each with 50% occupancy, was used to represent the disorder of these fluorine atoms. At the end of refinement[11] several peaks of about 1 e/Å^3 were found near the coordinated trifluoroacetate. These peaks, along the O1 and C23 resulted in a model in which the trifluoroacetate is disordered between two positions in a 4:1 ratio, with the coordinated oxygen O1 and C23 common to the two models. All non-hydrogen atoms were refined with anisotropic thermal parameters except the disordered trifluoroacetate atoms with 20% occupancy, which were assigned isotropic temperature factors. The hydrogen atoms were placed at calculated positions[11] (X–H, 0.95 Å) and allowed to "ride" on the atom to which they were attached. A common isotropic temperature factor for all hydrogen atoms was included in the refinement (U = 0.15 (1)).

The quantity $\sum w(|F_o| - |F_c|)^2$, where $w = 1.7962/(\sigma(F_o)^2 + 0.001\,498(F_o)^2)$ was minimized in the least-square refinement. During the final least-squares cycle, the shift in each parameter was less than 0.04 of its error. The final value for R is 0.079, and the final weighted discrepancy index R_w is 0.096.

Final non-hydrogen atomic positional parameters are given in Table II, and a list of interatomic distances and angles is given in Table III. A listing of observed and calculated structure factors is supplied in Table S1, and the final thermal parameters for non-hydrogen atoms are given in Table S2. Hydrogen atom parameters are listed in Table S3. Bond distances and angles within the ethylenediamine and trifluoroacetate ligands and the hexafluorophosphate counterion are listed in Table S4. (Tables S1–S4 are given as supplementary material.)

Results

Description of the Structure. A view of the cation, along with the atom labeling scheme, is given in Figure 1. The cation consists of a cobalt(III) coordinated to the four nitrogen atoms of two ethylenediamine ligands which are trans to one another and form an equatorial plane. The average Co–N bond distance is 1.944 (13) Å. The cobalt extends its coordination sphere to six by the axial coordination, Co–C = 1.922 (9) Å, of the carbon of an ethoxycarbonyl group ($CO_2C_2H_5^-$) and the oxygen, Co–O = 2.046 (7) Å, of a trifluoroacetate group. The cobalt atom lies in the plane (±0.03 Å) of the four coordinated ethylenediamine nitrogen atoms. Several weak intramolecular hydrogen bonds are formed

(11) Sheldrick, G. M. In *Shelx-76, Computing in Crystallography*; Shenk, H., Olthof-Hazekamp, R., van Koningsveld, H., Bassi, G. C.; Eds.; Delft University: Delft, Holland, 1978; pp 34–42.

Table II. Final Positional Parameters for the Non-Hydrogen Atoms in $[Co(en)_2(CF_3CO_2)(C(O)OC_2H_5)]PF_6$[a]

atom	*x*	*y*	*z*
Co	0.37796 (14)	0.20971 (8)	0.44388 (10)
N1	0.2015 (8)	0.2137 (5)	0.3537 (6)
C1	0.0940 (15)	0.1573 (10)	0.3928 (11)
C2	0.1674 (14)	0.0864 (7)	0.4425 (10)
N2	0.2934 (8)	0.1178 (4)	0.5132 (6)
N3	0.5619 (8)	0.2061 (5)	0.5270 (6)
C3	0.6713 (12)	0.2613 (8)	0.4794 (10)
C4	0.5882 (13)	0.3350 (7)	0.4374 (9)
N4	0.4652 (9)	0.3026 (4)	0.3738 (6)
C11	0.2966 (10)	0.2822 (6)	0.5439 (8)
O11	0.3042 (7)	0.2706 (4)	0.6353 (5)
O22	0.2336 (8)	0.3460 (4)	0.5009 (5)
C22	0.1759 (14)	0.4146 (9)	0.5621 (11)
C33	0.0212 (18)	0.3981 (9)	0.5806 (12)
O1	0.4683 (8)	0.1362 (4)	0.3350 (6)
O2	0.5682 (16)	0.0384 (7)	0.4265 (8)
C13	0.5393 (14)	0.0777 (9)	0.3445 (12)
C23	0.6015 (18)	0.0396 (10)	0.2463 (11)
F21	0.6296 (19)	−0.0346 (6)	0.2571 (10)
F22	0.5072 (15)	0.0337 (9)	0.1669 (9)
F23	0.711 (2)	0.0808 (15)	0.2094 (19)
F24	0.603 (6)	0.096 (3)	0.170 (3)
F25	0.737 (5)	0.023 (3)	0.298 (3)
F26	0.625 (10)	0.003 (5)	0.166 (6)
P	−0.0993 (4)	0.3669 (2)	0.2138 (2)
F1	−0.1487 (10)	0.3858 (5)	0.0993 (5)
F2	−0.0663 (9)	0.3437 (7)	0.3270 (6)
F3	−0.174 (8)	0.291 (2)	0.225 (2)
F4	−0.007 (3)	0.4561 (14)	0.197 (2)
F5	−0.228 (4)	0.426 (3)	0.230 (3)
F6	0.060 (5)	0.332 (2)	0.185 (3)
F7	−0.264 (2)	0.331 (4)	0.2220 (18)
F8	0.048 (4)	0.392 (3)	0.207 (3)
F9	−0.151 (5)	0.4407 (13)	0.263 (2)
F10	−0.046 (3)	0.282 (2)	0.1659 (19)
O2′	0.577 (4)	0.183 (2)	0.221 (3)
C13′	0.542 (7)	0.118 (4)	0.271 (5)

[a] Numbers in parentheses are errors in the last significant digit(s). Atoms F3 to F10 have an occupancy factor of 0.5. Atoms O2′, C13′, F24, F25, and F26 have an occupancy factor of 0.2, and atoms O2, C13, F21, F22, and F23 have an occupancy factor of 0.8.

Table III. Bond Distances (Å) and Angles (deg) for $[Co(en)_2(CO_2C_2H_5)(O_2C_2F_3)]PF_6$

	Cobalt–Ligand Distances		
Co–N1	1.946 (7)	Co–C11	1.922 (9)
Co–N2	1.925 (7)	Co–O1	2.046 (7)
Co–N3	1.952 (7)		
Co–N4	1.953 (7)		
	Cobalt–Ligand Angles		
N1–Co–N2	88.4 (3)	N3–Co–N4	85.7 (3)
N1–Co–N3	176.6 (3)	N3–Co–C11	89.5 (4)
N1–Co–N4	92.0 (4)	N3–Co–O1	90.2 (3)
N1–Co–C11	93.1 (4)	N4–Co–C11	90.2 (3)
N1–Co–O1	87.2 (3)	N4–Co–O1	87.7 (3)
N2–Co–N3	93.9 (3)	C11–Co–O1	177.9 (3)
N2–Co–N4	179.6 (2)		
N2–Co–C11	90.0 (4)		
N2–Co–O1	92.1 (3)		
	Ethoxyformyl Anion Distance and Angles		
C11–O11	1.196 (9)	Co–C11–O11	123.9 (7)
C11–O22	1.306 (10)	Co–C11–O22	112.5 (7)
O22–C22	1.481 (12)	O11–C11–O22	123.7 (9)
C22–C33	1.458 (18)	C11–O22–C22	122.6 (9)
		O22–C22–C33	108 (1)

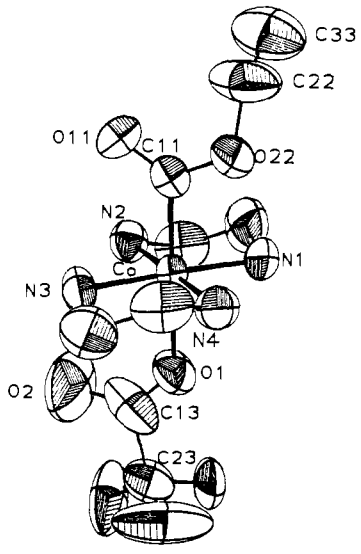

Figure 1. ORTEP view of the *trans*-$Co(en)_2(CO_2C_2H_5)(O_2CCF_3)^+$ cation showing the atom labeling scheme. The thermal ellipsoids are shown at the 50% probability level, with the hydrogen atoms omitted for clarity. Weak intramolecular hydrogen bonding occurs between the uncoordinated oxygen atoms of the ethoxycarbonyl and trifluoroacetate ligands and the amines of the ethylenediamine ligands.

Table IV. Hydrogen Bonding in $[Co(en)_2(CO_2C_2H_5)(O_2C_2F_3)]PF_6$[a]

	D–H	H···A	D···A	∠D–H···A
N1–H11···O11[b]	0.95	2.15 (1)	3.01 (1)	150.5 (2)
N1–H12···O22	0.95	2.38 (1)	2.89 (1)	113.8 (2)
N2–H21···O11	0.95	2.38 (1)	2.96 (1)	118.4 (2)
*N2–H22···O2	0.95	2.36 (2)	3.06 (2)	131.0 (3)
*N2–H22···O2[c]	0.95	2.07 (2)	2.94 (2)	152.6 (3)
N3–H31···O2	0.95	2.29 (1)	3.04 (1)	135.2 (3)
*N3–H32···O11	0.95	2.39 (1)	2.97 (1)	118.9 (2)
*N3–H32···O2′[d]	0.95	2.24 (4)	3.10 (4)	150 (1)
N4–H41···O22	0.95	2.34 (1)	2.81 (1)	110.1 (2)
N4–H42···O2′	0.95	2.16 (4)	2.98 (4)	145 (1)

[a] Asterisks indicate bifurcated hydrogen bond. [b] $x, {}^1/_2 - y, -{}^1/_2 + z$. [c] $1 - x, -y, 1 - z$. [d] $x, {}^1/_2 - y, {}^1/_2 + z$.

between the ethylenediamine hydrogens and the oxygen atoms of the ethoxycarbonyl and trifluoroacetate groups (see Table IV). The trifluoroacetate anion appears to be coordinated through the carbonyl oxygen (C=O, 1.159 (13) Å) rather than through the deprotonated oxygen (C–O⁻, 1.258 (15) Å) in a manner similar to the coordination of the protonated acetic acid in $V_3(\mu_3\text{-}O)(CH_3CO_2)_6(CH_3COOH)_2THF][VCl_4(CH_3COOH)_2]$.[12] In the present case this type of coordination is probably a result of the stronger intermolecular and intramolecular hydrogen bonds, which can be formed by the uncoordinated C–O⁻ oxygen versus those which could be formed if the coordination were through this oxygen atom and the carbonyl oxygen were free.

The bond distances within the coordinated ethoxycarbonyl ligand are similar to the corresponding distances found in the coordinated methoxycarbonyl of the complex $(CH_3OC(O))Co(CO)_3(PPh_3)$.[13] The Co–O1 distance of 2.046 (7) Å of the coordinated trifluoroacetate is much longer than the Co^{III}–O (trifluoroacetate) bond (1.936 (5) Å) found in $Co(C_6H_{16}N_2)_2(CF_3CO_2)_2](CF_3CO_2)$,[14] but it is about the same length as that found in complexes where Co(II)[15] is coordinated to trifluoroacetate. This is consistent with the group being weakly coordinated in **2** and with a strong trans effect of the ethoxycarbonyl ion. The Co–C bond length observed here (1.922 (9) Å) is significantly

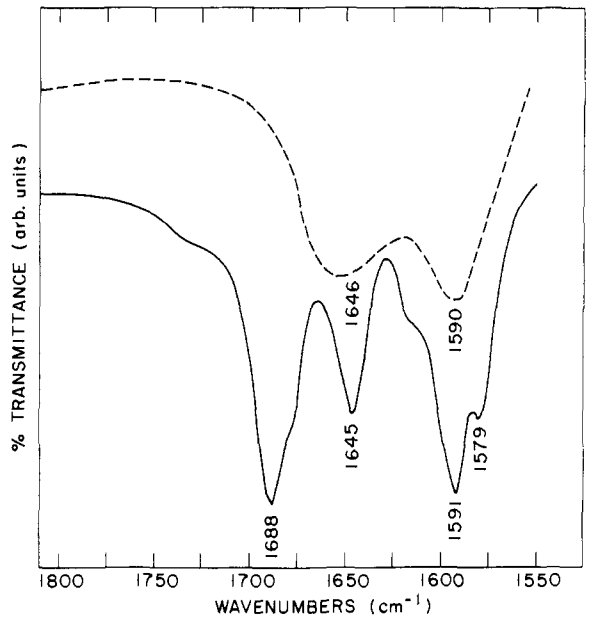

Figure 2. IR spectrum in the $\nu_{C=O}$ region of $[Co(en)_2(CO_2C_2H_5)(CF_3CO_2)](PF_6)$ (—) and of $[Co(en)_2(CO_2C_2H_5)(H_2O)](PF_6)_2$ (---) (as KBr pellets).

Table V. Comparison of $\nu_{C=O}$ Frequencies for Alkoxycarbonyl Complexes (KBr Pellets Unless Otherwise Noted)

compd	ν, cm^{-1}	ref
$[Co(CO)_3(P(OC_6H_5)_3)(CO_2C_2H_5)]$	1666 s	*a*
$[Co(CO)_2(P(C_6H_5)_3)_2(CO_2CH_3)]$	1633 s	*a*
$[Rh(CO)(Sb(C_6H_5)_3)_3(CO_2CH_3)]$	1621 s	*b*
$[IrCl_2(CO)(PMe_2Ph)_2(CO_2C_2H_5)]$	1663	*c*
$[IrCl_2(CO)(AsMe_2Ph)_2(CO_2C_2H_5)]$	1664	*c*
$[IrI_2(CO)(bpy)(CO_2C_2H_5)]$	1645	*d*
$[Cp^*Co(dppe)(CO_2C_2H_5)]BF_4$	1635	*e*
$[CpCo(dppe)(CO_2C_2H_5)]PF_6$	1625	*e*
$[Co(en)_2(CF_3CO_2)(CO_2C_2H_5)]PF_6$	1645 m	*f*
$[Co(en)_2(OH_2)(CO_2C_2H_5)](PF_6)_2$	1645 s	*f*

[a] Heiber, W.; Duchatsch, H. *Chem. Ber.* **1965**, *98*, 1744. [b] In THF: Heiber, W.; Frey, V. *Chem. Ber.* **1966**, *99*, 2614. [c] Nujol: Deeming, A. J.; Shaw, B. L. *J. Chem. Soc. A* **1969**, 443. [d] Malatesta, L.; Angoletta, M.; Caglio, G. *J. Chem. Soc. A* **1970**, 1836. [e] Bao, Q.-B.; Rheingold, A. L.; Brill, T. B. *Organometallics* **1986**, *5*, 2259. [f] This work.

shorter than the 1.971 (6)–1.99 (2)-Å distances found when[12] Co is coordinated to a $-CH_3$,[16] $-CO_2Me$[13], diethoxybutanoyl,[17] or $-C_2H_5$[18] group or the 2.00 (2)[19] and 2.06 (6)[20] distances found for Co(I) coordination to CO_2 (CO_2H). Bond distances within the en and $CF_3CO_2^-$ ligands are similar to those found in other complexes.[12,21]

All of the amine hydrogens on the en ligands are involved in either weak intramolecular or stronger intermolecular hydrogen bonds or in bifurcated hydrogen bonds (Table IV). The crystal lattice is held together by intermolecular hydrogen bonding between the en hydrogens and O2 of the $CF_3CO_2^-$ ion and O11 of the $-C(O)OC_2H_5$ group. A bifurcated hydrogen bond, one intramolecular and one intermolecular, is formed between an en hydrogen and two O2 atoms related by the inversion center (see Table IV). This results in an O2···O2* contact of 2.63 (1) Å. The

(12) Cotton, F. A.; Lewis, G. E.; Mott, G. N. *Inorg. Chem.* **1982**, *21*, 3316.
(13) Milstein, D.; Huckaby, J. L. *J. Am. Chem. Soc.* **1982**, *104*, 6150.
(14) Betran, F. G.; Capilla, A. V.; Aranda, R. A. *Cryst. Struct. Commun.* **1979**, *8*, 87.
(15) Alcock, N. W.; Atkins, M. P.; Golding, B. T.; Sellars, P. J. *J. Chem. Soc., Dalton Trans.* **1982**, 337.
(16) Heeg, M. L.; Endicott, J. F.; Glick, M. D. *Inorg. Chem.* **1981**, *20*, 1196.
(17) Tso, C. C.; Cutler, A. R.; Kullnig, R. K. *J. Am. Chem. Soc.* **1987**, *109*, 5844.
(18) Bakac, A.; Espenson, J. H. *Inorg. Chem.* **1987**, *26*, 4353.
(19) Gambarotta, S.; Arena, F.; Floriani, C.; Zanazzi, P. F. *J. Am. Chem. Soc.* **1982**, *104*, 5082.
(20) (a) Fujita, E.; Szalda, D. J.; Creutz, C.; Sutin, N. *J. Am. Chem. Soc.* **1988**, *110*, 4870. (b) Creutz, C.; Schwarz, H. A.; Wishart, J. F.; Fujita, E.; Sutin, N. *J. Am. Chem. Soc.* **1989**, *111*, 1153.
(21) Miskelly, G. M.; Clark, C. R.; Simpson, J.; Buckingham, D. A. *Inorg. Chem.* **1983**, *22*, 3237.

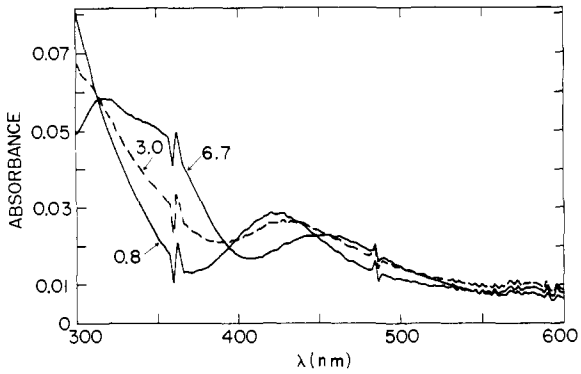

Figure 3. Absorption spectra of $Co(en)_2(OH_2)(CO_2H)^{2+}$ at pH 0.8, 3.0, and 6.7 at 15 °C. Near pH 3 the solutions undergo rapid decomposition. Thus the spectra were obtained within about 30 s of mixing with use of the HP diode array spectrometer.

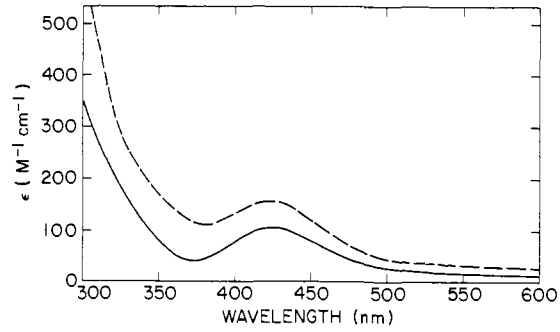

Figure 4. Absorption spectrum of $Co(en)_2(OH_2)(CO_2Et)^{2+}$ (solid line, pH 4 acetate buffer) and $Co(en)_2(OH)(CO_2Et)^{+}$ (dashed line, pH 9.8 carbonate buffer) at 25 °C.

fluorine atoms of the PF_6^- and the $CF_3CO_2^-$ are packed near one another and are probably responsible for disordering one another.

Characterization of the Complexes. Although crystals of the ethoxycarbonyl complex always contain bound $CF_3CO_2^-$, trifluoroacetate anion is not strongly bound in water. This was established by dissolving the solid $[Co(en)_2(CF_3CO_2)(C(O)OC_2H_5)]PF_6$ in water, quickly passing the solution through a cation-exchange column (onto which the cobalt complex adsorbed) and subjecting the effluent to anion analysis. The solution was found to contain $CF_3CO_2^-$ and PF_6^- in a 1:1 ratio. Thus, in what follows, it is assumed that the dominant form of the ester complex in aqueous solutions contains a water (or hydroxide) ligand trans to the Co–C bond. The rapid (<3 min) release of $CF_3CO_2^-$ in water was used to prepare the solid $[Co(en)_2(H_2O)(CO_2Et)](PF_6)_2$ for IR studies. Comparison of the IR spectrum of the latter with that of the trifluoroacetate-containing material (Figure 2) leads to the assignment of the 1645-cm^{-1} band to $\nu_{C=O}$ in the –C(O)OEt ligand. The C=O stretching frequencies of related alkoxycarbonyl complexes are compared in Table V. Additional significant frequencies include the following (cm^{-1}; KBr pellet): 1688 s ($\nu_{CO_2}^{as}$ of $CF_3CO_2^-$), 1645 m ($\nu_{C=O}$ of CO_2Et), 1591 s (δ_{NH_2} of en), 1203 s (CF_3 stretch), 1078 s (antisymmetric stretch of C–O–C group), 840 vs (ν_{PF}^{as} of PF_6^-). The ^1H NMR of a CD_3CN solution prepared from the crystals used in the diffraction studies confirms the integrity of the –C(O)OEt group in solution (values of δ relative to TMS): 1.29 (t, 3 H, $-CH_3$, J = 7.1 Hz); 2.37 (m, 8 H, CH_2 of en), 2.90 (br, 4 H, $-NH_2$), 3.60 (br, 4 H, $-NH_2$); 4.44 (q, 2 H, $-OCH_2-$, J = 7.1 Hz). For free CH_3CH_2OH, at approximately the same concentration as the Co complex, values of δ were: 1.10 (t, 3 H, $-CH_3$, J = 7 Hz); 2.65 (s, 1 H, –OH); 3.52 (q, 2 H, $-CH_2$, J = 7 Hz).

UV–vis absorption spectra of the metallocarboxylate **1** and its ester **2** are presented in Figures 3 and 4. The similarity of the spectra of the ester and the protonated metallocarboxylic acid is to be noted. The spectra of both **1** and **2** are a function of pH. In acidic solutions **1** exhibits an absorption maximum at 422 nm;[6] in the range pH 2–4 the band diminishes somewhat in intensity

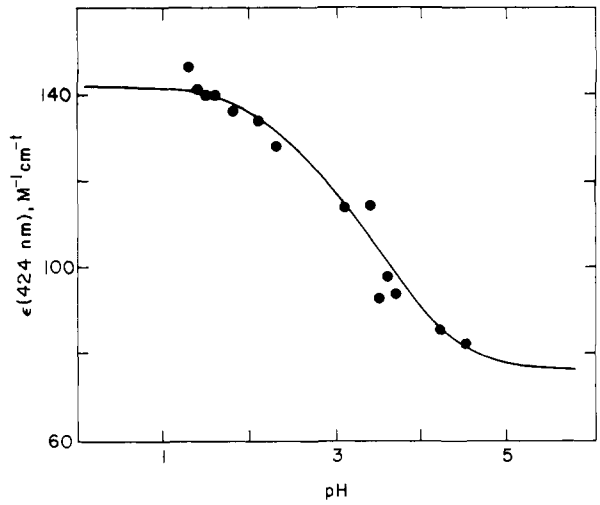

Figure 5. Spectrophotometric titration of $Co(en)_2(H_2O)(CO_2H)^{2+}$ at 15 °C and μ = 0.5 M. The solid line is calculated with pK_1 = 2.5 and pK_2 = 3.7. Near pH 3 the solutions undergo rapid decomposition. Thus the data were obtained within about 30 s of mixing with use of the HP diode array spectrometer.

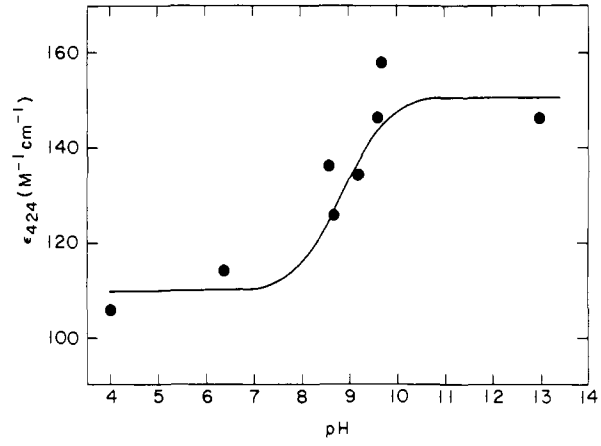

Figure 6. Spectrophotometric titration of $Co(en)_2(H_2O)(CO_2C_2H_5)^{2+}$ at 25 °C and μ = 0.5 M ($NaClO_4$). The solid line is calculated for pK_a = 8.7.

and shifts to longer wavelength. Above pH 5 the spectrum is pH independent with λ_{max} 450 nm. The absorption data presented in Figure 5 are consistent with eq 1 and 2 with pK_a values of 2.5

$$(H_2O)Co(en)_2(CO_2H)^{2+} \rightleftharpoons (H_2O)Co(en)_2(CO_2)^{+} + H^{+} \quad (1)$$

$$(H_2O)Co(en)_2(CO_2)^{+} \rightleftharpoons (HO)Co(en)_2(CO_2) + H^{+} \quad (2)$$

± 0.5 and 3.7 ± 0.5 for eq 1 and 2, respectively, at 15 °C and 0.5 M ionic strength. The data in Figure 5 are also consistent with a single pK_a value of 3.2, but the fit shown is suggested by the pH dependence of the kinetics (to be described). The fact that the complex is doubly charged[6] at pH ≤ 1 and uncharged at pH ≥ 7 is confirmed by its behavior on a cation-exchange column (see the Experimental Section). The spectrum of the ethoxycarbonyl complex **2** does not change over the range pH 0–7. However, at higher pH, small but reproducible intensity changes in the 300–400-nm region are found. As shown in Figure 6, these are consistent with a pK_a of 8.7 ± 0.2 for eq 3. In HCl solutions

$$(H_2O)Co(en)_2(CO_2Et)^{2+} \rightleftharpoons (OH)Co(en)_2(CO_2Et)^{+} + H^{+} \quad (3)$$

(4–12 M) the absorption maxima of both **1** and **2** shift to 428 nm, probably because of binding of Cl^- to the position trans to the Co–C bond. Absorption maxima and molar absorptivities for the species are summarized in Table VI.

Reactivity Patterns. $Co(en)_2(H_2O)(CO_2H)^{2+}$. As delineated by Vaudo et al.,[6] the decomposition of **1** to Co_{aq}^{2+} and CO_2 is

Table VI. Electronic Absorption Spectra (in Water, 25 °C Unless Otherwise Noted)

complex	λ_{max}, nm (ϵ, M^{-1} cm^{-1})
$Co(en)_2(CH_3CN)(CO_2Et)^{2+}$ [a]	410 (125), 314 sh (580), 262 (5200)
$Co(en)_2(H_2O)(CO_2Et)^{2+}$ [b]	424 (113), 320 sh (210), 264 (5100)
$Co(en)_2(OH)(CO_2Et)^{+}$ [c]	430 (159), 329 sh (260)
$Co(en)_2(H_2O)(CO_2H)^{2+}$ [d]	422 (140), 320 sh (300), 264 (6000)[5]
$Co(en)_2(OH)(CO_2)^{0}$ [e]	450 (100), 357 (245), 318 (280), 266 (9000)

[a] In acetonitrile solvent. [b] In 0.1 M CF_3SO_3H. In water (pH 5.8): 424 (106), 320 sh (206), 264 (4500), 208 (11 800). [c] At pH 9.72 (0.5 M ionic strength; carbonate/borate buffer). [d] In 0.1 M H_2SO_4, pH 1.35 (0.5 M ionic strength with $LiClO_4/Na_2SO_4$), 15 °C. [e] At pH 6–7 (0.03 M phosphate, 0.06 M $NaClO_4$), 25 °C.

Table VII. Pseudo-First-Order Rate Constants for Decomposition of $Co(en)_2(H_2O)(CO_2H)^{2+}$ at 25 °C and 0.5 M Ionic Strength ($NaClO_4$)[a]

conditns	k_{obsd}, s^{-1}
0.5 M $HClO_4$	2.1×10^{-5}
0.5 M $HClO_4$ (O_2 saturated)	2.2×10^{-5}
0.1 M $HClO_4$	3.4×10^{-5}
0.1 M HCO_2^-, pH 1.9[b]	4.0×10^{-4}
0.1 M $CH_3CO_2^-$, pH 3.2	2.55×10^{-3}
0.1 M $CH_3CO_2^-$, pH 3.2, $[Co(NH_3)_5Cl^{2+}] = 0.7$ mM[c]	2.43×10^{-3}
0.1 M HCO_2^-, pH 3.88[d,e]	1.95×10^{-3}
0.1 M HCO_2^-, pH 3.85	2.31×10^{-3}
0.1 M $CH_3CO_2^-$, pH 3.80[f]	2.50×10^{-3}
0.1 M HCO_2^-, pH 3.88, $[Co(NH_3)_5Cl^{2+}] = 0.7$ mM[c]	2.27×10^{-3}
0.1 M $CH_3CO_2^-$, pH 5.15	1.20×10^{-4}
0.1 M $CH_3CO_2^-$, pH 5.32	9.7×10^{-5}
0.1 M $CH_3CO_2^-$, pH 5.67	1.22×10^{-5}
0.1 M $CH_3CO_2^-$, pH 5.70	1.16×10^{-5}
0.1 M PO_4, pH 6.35	1.9×10^{-5}
0.1 M PO_4, pH 10.6[b]	1.2×10^{-7}

[a] (0.1–0.3) mM $Co-CO_2$ prepared by Method A (see the Experimental Section), monitored at 260 nm, argon-saturated solutions. [b] 1 mM $CoCO_2$, monitored at 420 or 450 nm. [c] >77% of $Co(NH_3)_5Cl^{2+}$ recovered at end of run. [d] Under 1 atm of CO_2. [e] Added 0.01 M ethylenediamine. [f] Under 10% CO_2 in Ar.

inhibited by acid at pH 1–3: pH 1 solutions have a half-life of ca. 2.5 h, but solutions near pH 3 have a half-life of only ca. 3.5 min. Although it was reported[6] that rapid base hydrolysis, yielding the dihydroxy complex $Co(en)_2(OH)_2^+$, occurs at pH > 9, we have found that this product actually arises from air oxidation: $Co(en)_2(OH)(CO_2)$ is oxidized to CO_2 + Co(III) rather rapidly by O_2 (k = 3 M^{-1} s^{-1} at 25 °C, based on runs with 0.0, 0.2, and 1.0 mM O_2, pH 5–7, $[Co-CO_2] = 3 \times 10^{-5}$ M). We did not investigate this reaction in detail but instead reinvestigated the decay kinetics and products as a function of pH in deaerated solutions. The disappearance of the complex was first-order in the complex at low concentrations ($\leq 2 \times 10^{-4}$ M) under all conditions. As shown in Tables VII and VIII, the rate was unaffected by added CO_2 (3×10^{-4}–3×10^{-2} M), added ethylenediamine (0.01 M), $Co(NH_3)_5Cl^{2+}$ (0.7 mM), and N_2O (ca. 0.02 M). In general the same k_{obsd} values were obtained at a given pH for the more concentrated solutions (ca. 1 mM). However, in a few runs (under argon but *not* under N_2O) with ca. 2 mM complex at pH 3–4, a large absorbance increase was observed throughout the spectrum a few minutes after initiating the run. These solutions had a grayish hue and scattered light. The anomalous "absorption" dissipated over several days. As discussed later, we suspect this behavior is due to formation of cobalt(0). In any event it precluded the determination of reliable kinetic data in only a few cases. The pseudo-first-order rate constants determined in the "well-behaved" runs are listed in Tables VII and VIII and plotted vs pH in Figure

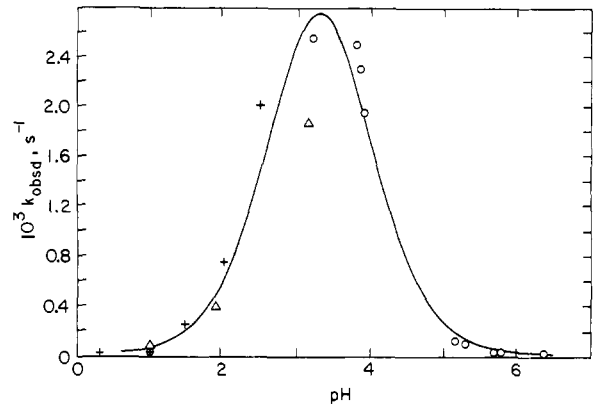

Figure 7. Pseudo-first-order rate constant for decomposition of $Co(en)_2(H_2O)(CO_2H)^{2+}$ as a function of pH at 25 °C. The curve is calculated for eq 4 with $a = 4.5 \times 10^{-3}$ s^{-1}, $b = 1.58 \times 10^{-4}$ M ($pK_2 = 3.8$), and $c = 1.58 \times 10^{-3}$ M ($pK_1 = 2.8$). The triangles were obtained at ~1 mM initial $Co-CO_2$ concentration (Table VIII), the circles, at 0.3 mM initial $[Co-CO_2]$ (Table VII), and the crosses, from ref 6.

Table VIII. Products of $Co(en)_2(H_2O)(CO_2H)^{2+}$ Decomposition at 25 °C[a]

pH	$[Co-CO_2]_0$, mM	k_{obsd}, s^{-1}	product yield					
			CO_2	CO	H_2	HCO_2^-	$C_2O_4^{2-}$	H_2CO
0.82[b]	0.22		0.81		0.06			≤0.01
0.85[b]	0.73		0.73	0.06	0.13	<0.01	<0.05	
0.85[b–e]	1.8	5.2×10^{-5}	0.99	0.07	0.03			
1.00[b,c]	2.0	6.6×10^{-5}	1.03	0.07	0.12			
1.75	0.73		1.06	0.06	0.15			
2.07	0.22		0.83		0.19			≤0.01
3.03	0.22		0.85		0.11			
3.15[f]	0.73	1.9×10^{-3}	0.80	0.07	0.11	0.03	≤0.05	≤0.01
3.60	0.73		1.1		0.3			
3.60[d,g,h]	2.0	2.3×10^{-3}	1.01	0.08	0.08			
3.8[d,e,i]	0.25	2.2×10^{-3}	1.04	0.08	0.01			
6.37	2.2	4.0×10^{-6}	0.87	0.02	0.01			
(12)[j]	1.4	$<1 \times 10^{-8}$						
[HCl]								
4 M[k]	1.7	2.3×10^{-5}	0.06	0.31	0.02			
4 M[l]	0.0		<0.01	<0.01	<0.01			
6 M[k]	1.2	4.7×10^{-5}	0.37	0.89	0.26			
6 M[l]	0.0		<0.01	<0.01	<0.01			
8 M[k,m]	1.2	7.2×10^{-5}	0.26	0.74	0.19			
8 M[l]	0.0		0.02	<0.01	<0.01			

[a] Stock $Co(en)_2(OH)CO_2$ solutions were prepared by Method B (see the Experimental Section). Yield = moles of product/mole of $Co-CO_2$ taken. All solutions are argon-saturated and contain 0.03 M phosphate and 0.06 M $NaClO_4$, μ = 0.10–0.15 M and Co(II) yield ≥0.95 unless otherwise noted. Errors on gas yields are estimated to be ±15% of value reported. [b] –log $[HClO_4]$. [c] μ = 0.3 M. [d] Solution saturated with N_2O. [e] Yield N_2 = 0.53. [f] Yield $CH_4 \leq 0.01$. [g] Contained 0.08 M formate buffer and stock solution prepared by Method A. [h] Yield N_2 = 0.56. [i] Total phosphate concentration is 0.23 M. [j] Estimated from the behavior of the product solution for 0.01 M NaOH in Table IX. [k] Cobalt product is *cis*-$Co(en)_2Cl_2^+$/*trans*-$Co(en)_2Cl_2^+$ mixture. [l] Contained 2 mM $NaHCO_2$; analyzed after 5 days. [m] Co(II) yield < 0.01 based on $CoCl_4^{2-}$.

Table IX. Decomposition of $Co(en)_2(H_2O)(CO_2Et)^{2+}$ at 22 ± 2 °C[a]

pH	solution	k_{obsd}, s^{-1}	product yield			
			CO_2	CO	H_2	Co(II)
(1)[b]	0.1 M $HClO_4$	2.5×10^{-6}	0.97	<0.1	<0.1	1.03
(1.7)	0.02 M $HClO_4$	4.6×10^{-7}	0.58	0.09	<0.1	0.91
5.5	0.02 M PO_4 total	2.2×10^{-7}	0.65	0.01	0.03	0.97
6.2	0.02 M Ac total	1.6×10^{-7}	0.79[c]	0.01[c]	0.02[c]	
7.0	0.02 M PO_4 totat	$\leq 2 \times 10^{-7}$	*d*			
8.8	0.02 M PO_4 total	$\leq 2 \times 10^{-8}$				
10.6	0.02 M PO_4 total	2.7×10^{-7}	*e*			
(12)	0.01 M NaOH	5.9×10^{-7}	*e*			
(13)	0.1 M NaOH	$\sim 3 \times 10^{-6}$	*e*,*f*			
	6 M HCl[g]	4.0×10^{-5}	0.07	1.1	0.05	

[a] In most experiments, ~2 mg of solid ester was taken (~1.3×10^{-3} M), no supporting electrolyte was added, Na^+ salts of the buffers were used, and the disappearance was followed at 425 (pH 1–7), 430 (pH 8.8, 10.6), 350 (pH 12, 13), or 428 nm (6 M HCl). Analyses were carried out at >90% reaction. "Yield" is defined as moles of product per mole of $Co(en)_2(CO_2Et)$ taken. Errors on gas yields are estimated as ±15% of value given. [b] In 0.1 M CF_3SO_3H, $k_{obsd} \sim 5 \times 10^{-6}$ s^{-1}. Yields: C_2H_5OH, 1.07; HCO_2^-, 0.04; $C_2O_4^{2-}$, 0.04. [c] Analyzed after 60% reaction (70 days). Values reported have been normalized to 100% reaction. [d] λ_{max} shifts from 425 to 430 nm over 1500 h. [e] Product is $Co(en)_2(OH)(CO_2)$. [f] Yield C_2H_5OH = 1.0. [g] Product is $Co(en)_2Cl_2^+$.

7. From the bell-shaped curve, which exhibits a maximum rate at ca. pH 3.2, it is evident that the $[H^+]$ dependence is of the form given in eq 4. The solid curve shown in Figure 7 is calculated from eq 4 with $a = 4.5 \times 10^{-3}$ s^{-1}, $b = 1.58 \times 10^{-4}$ M, and $c = 1.58 \times 10^{-3}$ M.

$$k_{obsd} = a/(1 + b/[H^+] + [H^+]/c) \quad (4)$$

As reported by the earlier workers, Co_{aq}^{2+} is the only significant (>95%) cobalt product at pH 0–3; furthermore, in the absence of O_2, this is also the case at higher pH (even in fairly alkaline solutions, where, with phosphate buffers, a violet Co(II) precipitate results). The major carbon product in this pH range is CO_2 (or HCO_3^-/CO_3^{2-}). Carbon monoxide (≤10% of carbon) is also produced, but no significant quantity of oxalate is detected under any conditions. The only other major product is H_2 (up to 20% based on $Co-CO_2$ taken, mol/mol). As shown in Table VIII, >80% of the carboxylate carbon is accounted for (mainly as CO_2). For the pH 0–6.4 data, there is, however, a deficit in "reducing" equivalents. Since Co(II) is the only cobalt product, conservation of charge suggests that moles of $Co-CO_2$ taken = 2 × moles of $(H_2 + CO + C_2O_4^{2-} + HCO_2^-)$. At most this sum is less than 0.5. Thus other reduced carbon fragments were sought, but neither methane nor formaldehyde was detected. As noted earlier, some of the more concentrated solutions scattered light and may contain colloidal cobalt metal. If so, the Co(0) is oxidized by either air or the NH_4SCN solutions used in the Co(II) analyses since >95% of the cobalt is determined as Co(II) with the Kitson method. In contrast, when similar runs were carried out under nitrous oxide instead of argon (Table VIII), no light scattering was observed and N_2 was produced. As discussed later, N_2O is expected to intercept cobalt(I). In the presence of N_2O the observed yields are in good agreement with the stoichiometry in eq 5. This observation also suggests that disproportionation of Co(I) to Co(0) is responsible for the "electron deficit" in the absence of N_2O.

$$Co(en)_2(CO_2)^+ + 0.5N_2O + 5H^+ \rightarrow Co_{aq}^{2+} + 2enH_2^{2+} + CO_2 + 0.5N_2 + 0.5H_2O \quad (5)$$

By contrast, as reported in the earlier work,[6] in strongly acidic solutions (4–8 M HCl) the sole cobalt product is cobalt(III) (*cis*- and *trans*-$Co(en)_2Cl_2^+$) and the CO yield rises to ca. 80% of the carbon product, with some H_2 and CO_2 also being formed. The formate "blanks" shown at the bottom of Table VIII establish that CO does not arise from decarbonylation of free formic acid.[22] In these solutions the absorption maximum of the (reactant) complex is shifted to 428 nm, possibly because of replacement of the *trans*-water by chloride ion. The kinetics are first-order in $[Co-CO_2]$ in the concentrated HCl solutions, and rates increase with [HCl]. The product distributions as a function of conditions are given in Table VIII.

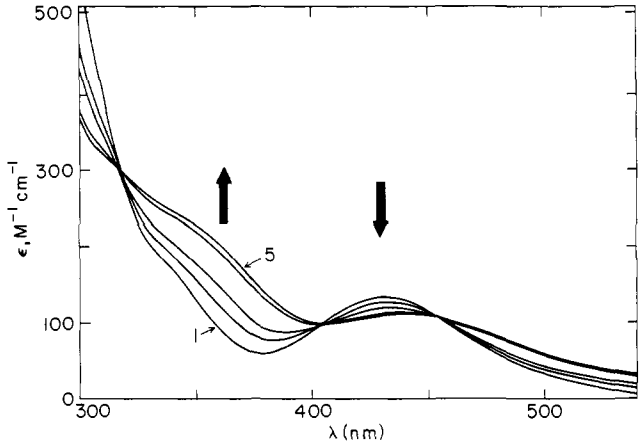

Figure 8. Hydrolysis of the ester function in $Co(en)_2(OH)(C(O)OEt)^+$ in deaerated 0.01 M NaOH (1.3 mM complex at 22 ± 2 °C). Traces 1–5 were obtained 0, 93, 189, 261, and 525 h after initiating the run.

$Co(en)_2(H_2O)(CO_2Et)^{2+}$. The reactivity of the ester **2** is markedly diminished in comparison to the parent complex over most of the pH range. At 22 ± 2 °C, the decay half-life is 4 days at pH 1, 50 days at pH 7, and about 3 days at pH 13. Under all conditions the decay of the metalloester absorption features is pseudo-first-order. At pH 1–7 the $[H^+]$ dependence is given by eq 6 with $d = 1.6 \times 10^{-7}$ s^{-1} and $e = 2.5 \times 10^{-5}$ M^{-1} s^{-1}. Above ca. pH 10 (where the reactant is $Co(en)_2(OH)(CO_2Et)^+$; eq 3) the rate is accelerated by hydroxide ion (eq 6b) with $f = 3.0 \times 10^{-5}$ M^{-1} s^{-1}. The products obtained are a function of pH. Table IX summarizes the results of the kinetics and product studies. At pH 0–8, the sole cobalt product is Co_{aq}^{2+}; however, at pH ≥ 11 the parent carboxylate $Co(en)_2(OH)(CO_2)$ is formed stoichiometrically (Figure 8). In strongly acidic (4–12 M HCl) solutions, the absorption maximum of the starting solution shifts to 428 nm, the decay is first-order in the complex, and Co^{III} ($Co(en)_2Cl_2^+$) and CO are products. Although the ester decomposition rates were not sensitive to air at pH 0–13, the products were: at pH 7 and 13, $Co(en)_2(OH)_2^+$ was observed as found earlier[6] for the carboxylate complex **1** under similar conditions. As discussed later, we attribute this to oxidation of $Co(en)_2(OH)(CO_2)$ (formed by hydrolysis of **2**) to Co(III).

$$k_{obsd} = d + e[H^+] \qquad pH \leq 7 \quad (6a)$$

$$k_{obsd} = f[OH^-] \qquad pH > 10 \quad (6b)$$

Discussion

The X-ray analysis (Figure 1) demonstrates that **2** is an η^1-C metalloester (ethoxycarbonyl) in the solid state. The ^1H NMR

(22) (a) Decarbonylation of formic acid occurs in concentrated sulfuric acid solutions.[22b] However, we find no evidence for this reaction at 25 °C over 5 days even in 12 M HCl. (b) See: Bowers, P. G.; Hodes, K. *J. Phys. Chem.* **1988**, *92*, 2489 and references cited therein.

Table X. Comparison of *trans*-$Co(en)_2X(H_2O)^{2+}$ Complexes

X^-	λ_{max}, nm (ϵ, M^{-1} cm^{-1})	$pK(H_2O)$
OH^a		7.94
Br^b	620 (34), 450 sh	
Cl^c	590 (28), 450 (32), 360 sh	5.8
F^d	575 (28), 450 (32), 350 (55)	
NCS^e	538 (185)	~7
NO_2^f		6.44
SO_3^{-g}	467 (164), 360 (98)	
CN^h	450 (80), 332 (65)	7.5
$-CO_2H^i$	422 (140), 320 sh (300)	
$-CO_2Et^i$	424 (113), 320 sh (210)	8.7

[a] Bjerrum, J.; Rassmussen, S. E. *Acta Chem. Scand.* **1952**, *6*, 1265. [b] Chan, S. C.; Tobe, M. L. *J. Chem. Soc.* **1962**, 4531. [c] Baldwin, M. E.; Chan, S. C.; Tobe, M. L. *J. Chem. Soc.* **1961**, 4637. [d] Chan, S. C.; Poon, C. K. *J. Chem. Soc. A* **1966**, 146. [e] Ardon, M.; Bino, A.; Jackson, W. G. *Polyhedron* **1987**, *6*, 181. [f] Basolo, F.; Stone, B. D.; Bergmann, J. G.; Pearson, R. G. *J. Am. Chem. Soc.* **1954**, *76*, 3079. [g] Jackson, W. G. *Inorg. Chem.* **1988**, *27*, 777. [h] Chan, S. C.; Tobe, M. L. *J. Chem. Soc.* **1963**, 966. [i] This work.

spectrum indicates that this coordination mode is retained in acetonitrile solution. The similarity of UV–vis spectra for aqueous and acetonitrile solutions is evidence that the coordination mode is preserved in aqueous media, as well. Furthermore, ^1H NMR studies of **2** in 0.1 M NaOD confirm that the en ligands are trans to one another under alkaline conditions.[23a] As for the parent metallocarboxylate complex **1**, its behavior,[6] the similarity of its spectrum (in acid) to that of **2**, and the fact that it reacts with ethanol under acidic conditions to yield **2** leave no doubt that it is an η^1-C metallocarboxylic acid.[23b,c] By analogous arguments **1** and **2** are assumed to have *trans*-ethylenediamine ligands in acidic aqueous solutions.

All of the physical evidence indicates that $-CO_2^{2-}$ and $-CO_2R^-$ are very strong field ligands. In $Co(en)_2(CF_3CO_2)(CO_2Et)^+$ the Co–C distance (1.922 (9) Å) is among the shortest reported while the *trans*-Co–O distance (2.046 (7) Å) is quite long. Comparison of the ligand field spectra of **1** and **2** with those of other *trans*-$Co(en)_2(H_2O)X^{2+}$ complexes (see Table X) suggests that $-CO_2H^-$ and $-CO_2Et^-$ rank even higher in the spectrochemical series than CN^-. On the basis of comparison of **1** and **2** with recently described carbon-bonded cobalt cyclam derivatives,[18] $-CO_2H^-$ and $-CO_2R^-$ also rank above $-CH_3^-$, $-CH_2Cl^-$, $-CH_2OCH_3^-$, etc., as well, for Co(III) bonded to entirely saturated amine ligands.

Our spectral studies (Figures 3 and 4) of the deprotonation of **1** suggest a pK_a of 2.5 ± 0.5 at 15 °C for the carboxylic acid function in **1** (eq 1). Because pK_1 and pK_2 are so close to one another, "pure" solutions of the intermediate 1+ species could not be obtained. Two tautomers of the singly deprotonated species, $Co(en)_2(H_2O)(CO_2)^+$ and $Co(en)_2(OH)(CO_2H)^+$, are possible. The former assignment is more appealing in light of the kinetics. In addition, this assignment provides a partial explanation for the large acidity of the bound water molecule ($pK \sim 4$). If the water ionized first, i.e. eq 1′, $pK_{1'}$ would be expected to be similar to that found for the ester derivative **2** ($pK_3 = 8.7 \pm 0.2$). Indeed,

$$Co(en)_2(H_2O)(CO_2H)^{2+} \overset{pK_{1'}}{\rightleftharpoons} Co(en)_2(OH)(CO_2H)^+ + H^+ \quad (1')$$

$$Co(en)_2(OH)(CO_2H)^+ \overset{pK_2}{\rightleftharpoons} Co(en)_2(OH)(CO_2) + H^+ \quad (2')$$

pK_3 is of the magnitude normally found for bound water on Co(III) complexes of this charge type (Table X). The high acidity of water bound trans to $-CO_2^{2-}$ (eq 2) could arise through resonance stabilization of the neutral product.

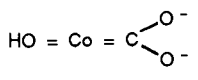

In any event the $-CO_2H$ function in **1** is a rather strong acid, a somewhat stronger acid than formic acid ($pK_a = 3.7$)[24] and *sec-dl*-5,7,7,12,14,14-hexamethyl-1,4,8,11-tetraazacyclotetradeca-4,11-dienecobalt hydroxycarbonyl dication.[20b] In its acidity, dispositive **1** is in striking contrast to $Ru(bpy)_2(CO)(CO_2H)^+$ ($pK = 9.6$)[25] and $(NC)_5FeCNCo(CN)_2(PEt_3)_2(CO_2H)^{4-}$ ($pK = 11.5$).[26] (Despite the relatively large number of metallocarboxylic acids known,[3a,27] the above four species appear to be the only ones for which equilibrium acidity values have been recorded.)

Our reinvestigation of the decomposition of $Co(en)_2(H_2O)(CO_2H)^{2+}$ yields results substantially in agreement with the earlier work[6] up to about pH 3. Above pH 3 the solutions ($Co(en)_2(OH)(CO_2)$) are O_2 sensitive; the high rates and Co(III) product reported in the earlier work at higher pH are undoubtedly due to the presence of air. At pH 1–8, the rates of disappearance of the complex in deaerated solutions are described by eq 4. This $[H^+]$ dependence is consistent with a rate-determining reaction of the singly protonated species $Co(en)_2(H_2O)(CO_2)^+$. Thus, in the rate law eq 4, c is identified with K_1 (eq 1), b is identified with K_2 (eq 2), and $a = 4.5 \times 10^{-3}$ s^{-1} at 25 °C is the rate constant for the rate-determining reaction of $Co(en)_2(H_2O)(CO_2)^+$.

We turn now to the nature of the rate-determining first-order reaction of $Co(en)_2(H_2O)(CO_2)^+$. Two possibilities must be considered: Scheme I, which involves reductive elimination of CO_2 to give $Co(en)_2^+$, and Scheme II, which involves reductive elimination of $^\bullet CO_2^-$ ("homolysis") to give $Co(en)_2^{2+}$. The operation of Scheme I has been established for the macrocyclic $CoL(CO_2)^+$ system[20] where L = *dl*-5,7,7,12,14,14-hexamethyl-1,4,8,11-tetraazacyclotetradeca-4,11-diene. Scheme II has been proposed for the present system[6] and for the NTA (nitrilotriacetate) complex[28] $Co(NTA)(CO_2)^{2-}$. The thermodynamic preference of a given system for Scheme I versus Scheme II—that is, the position of equilibrium 7—depends upon the Co(II)/Co(I) reduction potential. The CO_2/CO_2^- reduction potential is −1.90 V in water.[29] That for macrocyclic CoL^{2+}/CoL^+ (above) is ca. −1.4 V;[30] thus, for $CoL(CO_2)^+$, $K_7 \geq 10^8$ and Scheme I is favored substantially. Unfortunately, $E°$ data are not available for $Co(en)_2^{2+}/Co(en)_2^+$ (nor for $Co(NTA)^-/Co(NTA)^{2-}$). On the basis of data for saturated N_4 macrocycles,[30] the $E°$ for $Co(en)_2^{2+}/Co(en)_2^+$ could be as high as ca. −1.8 V (favoring Scheme I), but

Scheme I

$$Co(en)_2(H_2O)(CO_2)^+ \rightarrow Co(en)_2^+ + CO_2$$

$$Co(en)_2^+ \rightarrow \rightarrow Co_{aq}^{2+}$$

Scheme II

$$Co(en)_2(H_2O)(CO_2)^+ \rightarrow Co(en)_2^{2+} + {}^\bullet CO_2^-$$

$$Co(en)_2^{2+} \xrightarrow{H^+} Co_{aq}^{2+} + 2enH_2^{2+}$$

$$^\bullet CO_2^- \rightarrow \rightarrow \text{products}$$

(23) (a) Schwarz, C., work in progress. (b) Crystals of polymeric $[Co(en)_2(CO_2)(ClO_4)]_n$ have recently been obtained from water, and they contain *trans*-ethylenediamine groups.[23c] The CO_2^{2-} bridges two Co(III) centers, binding one through carbon and the other through oxygen in a repeating unit reminiscent of that in **2**. (c) Szalda, D., work in progress.

(24) Gordon, A. J.; Ford, R. A. *The Chemist's Companion*; Wiley: New York, 1972.
(25) Ishida, H.; Tanaka, K.; Morimoto, M.; Tanaka, T. *Organometallics* **1986**, *5*, 724.
(26) Bercaw, J. E.; Goh, L.-Y.; Halpern, J. *J. Am. Chem. Soc.* **1972**, *94*, 6534.
(27) For reviews, see ref 3a and Angelici, R. J. *Acc. Chem. Res.* **1972**, *5*, 335. (a) Grice, N.; Kao, S. C.; Pettit, R. *J. Am. Chem. Soc.* **1979**, *101*, 1627. (b) Catellani, M.; Halpern, J. *Inorg. Chem.* **1980**, *19*, 566. (c) Casey, C. P.; Andrews, M. A.; McAllister, M. A.; Rinz, J. E. *J. Am. Chem. Soc.* **1980**, *102*, 1927. (d) Sweet, J. R.; Graham, W. A. G. *Organometallics* **1982**, *7*, 982.
(28) Meyerstein, D.; Schwarz, H. A. *J. Chem. Soc., Faraday Trans. 1* **1988**, *84*, 2933.
(29) Schwarz, H. A.; Dodson, R. W. *J. Phys. Chem.* **1989**, *93*, 409.
(30) Tait, A. M.; Lovecchio, F. V.; Busch, D. H. *Inorg. Chem.* **1977**, *16*, 2206.

Scheme III

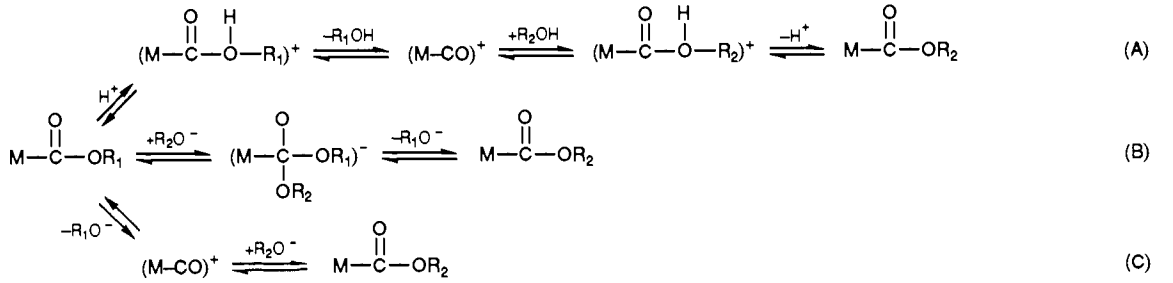

it is not clear that the macrocycles are a good model for the ethylenediamine couple. Thus we cannot use thermodynamic data to exclude one possibility or the other for $Co(en)_2(H_2O)(CO_2)^+$. The pH dependence of the rates is qualitatively consistent with either scheme: Protonation, giving $Co(en)_2(H_2O)(CO_2H)^{2+}$, destabilizes the carbon-based elimination products, CO_2H^+ (Scheme I) and $^\bullet CO_2H$ (Scheme II).[31] Deprotonation to $Co(en)_2(OH)(CO_2)$ destabilizes the metal-based elimination products, $Co^{I}(en)_2(OH)$ (Scheme I) and $Co^{II}(en)_2(OH)^+$ (Scheme II).

In principle, the product distribution and the influence of scavengers could clarify the nature of the rate-determining step. Scheme I is consistent with the high CO_2 yields, whereas the normal fate of the $^\bullet CO_2^-$ radical at pH > 2 would be formation of oxalate[32] via eq 8. Similarly, the results upon addition of nitrous

$$2^\bullet CO_2^- \rightarrow C_2O_4^{2-} \qquad k_8 = 7.5 \times 10^8\ M^{-1}\ s^{-1} \qquad (8)$$

oxide, which reacts rapidly with cobalt(I) complexes[33,34] but not[34] with $^\bullet CO_2^-$, would suggest that Scheme I predominates. However, both the high CO_2 yields and the formation of cobalt(I) could result from Scheme II and eq 9, oxidation of $^\bullet CO_2^-$ by Co_{aq}^{2+},

$$^\bullet CO_2^- + Co_{aq}^{2+} \rightarrow CO_2 + Co_{aq}^{+} \qquad (9)$$

which has been observed in γ-radiolysis experiments.[34] The uncertainties[34] in the earlier work are such that the operation of eq 9 in the present system cannot be ruled out. Whether Scheme I or Scheme II followed by eq 9 obtains, formation of H_2 (eq 10),

$$Co(en)_2(H_2O)(CO_2H)^{2+} + 5H^+ \rightarrow Co_{aq}^{2+} + 2enH_2^{2+} + CO_2 + \tfrac{1}{2}H_2 \qquad (10)$$

$$Co(en)_2^+ \text{ or } Co_{aq}^+ + H_3O^+ \rightarrow Co(en)_2(H)(H_2O)^{2+} \text{ or } Co(H)_{aq}^{2+} \qquad (11)$$

$$Co(en)_2(H)(H_2O)^{2+} \text{ or } Co(H)_{aq}^{2+} + H^+ \rightarrow Co_{aq}^{2+} + 2enH_2^{2+} + \tfrac{1}{2}H_2 \qquad (12)$$

arising from reaction of Co(I) with acid (e.g., eq 11, 12),[35] might have been expected. However, the H_2 yields are at most a factor of 2 below that expected from eq 10. Evidently, eq 12 is not efficient in this system, and Co(I) or the hydride complex (via Co(I)) undergoes disproportionation

$$2Co(I) \rightarrow Co(II) + Co(0)$$

giving rise to a fairly unreactive Co(0) species.[36] Finally, the effects of added scavengers are also ambiguous concerning the nature of the rate-determining step. However, these experiments do strongly suggest that the primary elimination event is irreversible. Since added CO_2 and added N_2O do not, respectively, inhibit and enhance the rate, Scheme I (if operative) is not a preequilibrium; similarly, the insensitivity of the rates to added $Co(NH_3)_5Cl^{2+}$ ($k_{13} = 1.5 \times 10^8\ M^{-1}\ s^{-1}$)[37a] and O_2 (at pH < 3; $k_{14} = 2 \times 10^9\ M^{-1}\ s^{-1}$)[37b] (eq 13, 14) establishes that Scheme II (if operative) is not a preequilibrium.

$$CO_2^- + Co(NH_3)_5Cl^{2+} \rightarrow CO_2 + Co^{2+} + 5NH_4^+ + Cl^- \qquad (13)$$

$$CO_2^- + O_2 \rightarrow CO_2 + O_2^- \qquad (14)$$

Decomposition of $Co(en)_2(OH_2)(C(O)OC_2H_5)^{2+}$. Between pH 1 and 8, the disappearance of the ester is 1–10 orders of magnitude slower than that of $Co(en)_2(OH_2)(CO_2H)^{2+}$. At pH > 11 the ester is converted cleanly to the carboxylate (Figure 8). Stoichiometric formation of ethanol is found at both pH 1 and 13. The distribution of other products of the ester decomposition (Co(II), CO_2, H_2, and CO) is within error identical with that found for the carboxylate. Thus we propose that hydrolysis of the ester function to give the carboxylate complex (eq 15) is the only

$$OH^- + Co(en)_2(H_2O)(CO_2Et)^{2+} \rightarrow Co(en)_2(H_2O)(CO_2)^+ + EtOH \qquad (15)$$

reaction that the ester undergoes under these conditions. The other products (Co(II), CO_2, etc.) are then determined by reactions of the carboxylate complex. Consistent with this hypothesis is the following: In contrast to the carboxylate complex, the ester complex does not react with oxygen; its decay rate is not accelerated in air-saturated solutions ($k_{O_2} < 10^{-4}\ M^{-1}\ s^{-1}$). However, the products obtained from alkaline O_2-free and air-saturated solutions of the ester are Co(II) and $Co(en)_2(OH)_2^+$, respectively, as found for the carboxylate. Thus, the rate of decomposition of the ester is determined by its hydrolysis rate, but the products (apart from ethanol) reflect the reactivity of the hydrolysis product, the metallocarboxylate.

We turn now to the mechanism for the hydrolysis of the ester ethoxycarbonyl function and the significance of eq 6. Scheme III summarizes possible hydrolysis routes. Scheme IIIC is suggested by the fact that alkoxycarbonyl complexes[27] are most commonly prepared via nucleophilic attack on bound CO (eq 16).

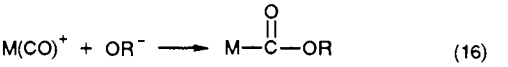

The reaction is favored[38] by high charge on the metal, electron-withdrawing groups on the other ligands, and little M–CO back-bonding (high $\nu_{C=O}$). The few equilibrium and kinetic data sets that exist[39-41] (eq 17–19) indicate that equilibration is in-

(31) Note that the pK_a of protonated formate radical $^\bullet C(O)(OH)$ is 1.4 as reported by: Buxton, G. V.; Sellers, R. M. *J. Chem. Soc., Faraday Trans. 1* **1973**, *69*, 555.

(32) Neta, P.; Simic, M.; Hayon, E. *J. Phys. Chem.* **1969**, *73*, 4207.

(33) Rapid reaction with N_2O is a relatively general characteristic of cobalt(I). See e.g.: Buxton, G. V.; Sellers, R. M. *Natl. Stand. Ref. Data Ser., (U.S. Natl. Bur. Stand.)* **1978**, *62*, 13–19.

(34) Buxton, G. V.; Dainton, F.; McCracken, D. R. *J. Chem. Soc., Faraday Trans. 1* **1973**, *69*, 243.

(35) (a) Conversion of $Co(en)_2^+$ to its conjugate acid $Co(en)_2(H)(H_2O)^{2+}$ is expected to be very rapid. Macrocyclic analogues of $Co(en)_2^+$ have been found to be rapidly protonated by H_2O.[35b] (b) Schwarz, H. A., unpublished work. (c) It is possible, however, that $Co(en)_2^+$ undergoes rapid en loss to give Co_{aq}^+.

(36) The water-induced precipitation of unreactive cobalt metal from Co(I) solutions in pyridine has recently been reported: Fachinetti, G.; Fanaioli, T.; Zanazzi, P. F. *J. Chem. Soc., Chem. Commun.* **1988**, 1100.

(37) (a) Hoffman, M. Z.; Simic, M. *Inorg. Chem.* **1973**, *12*, 2471. (b) Buxton, G. V.; Sellers, R. M.; McCracken, D. R. *J. Chem. Soc., Faraday Trans. 1* **1976**, *72*, 1464.

(38) See e.g.: Bao, Q.-B.; Rheingold, A. L.; Brill, T. B. *Organometallics* **1986**, *5*, 2259.

(39) Pearson, R. G.; Mauermann, H. *J. Am. Chem. Soc.* **1982**, *104*, 500.

(40) Gross, D. C.; Ford, P. C. *J. Am. Chem. Soc.* **1985**, *107*, 585.

(41) Ishida, H.; Tanaka, K.; Morimoto, M.; Tanaka, T. *Organometallics* **1986**, *5*, 724.

trinsically rather rapid. For example, for eq 18 $k_f = 2 \times 10^3$ M^{-1}

$$Fe(CO)_5 + OCH_3^- \rightleftharpoons Fe(CO)_4(C(O)OCH_3)^- \quad (17)$$

$$Ru_3(CO)_{12} + OCH_3^- \rightleftharpoons Ru_3(CO)_{11}(C(O)OCH_3)^- \quad (18)$$

$$Ru(bpy)_2(CO)_2^{2+} + OH^- \rightleftharpoons Ru(bpy)_2(CO)(C(O)OH)^+ \quad (19)$$

s^{-1}; $k_r = 2$ s^{-1}, and $K_{18} = 10^3$ M^{-1} in methanol at 25 °C. Thus the sequence given at the bottom of Scheme III provides one mechanism for "transesterification" (R_1 and R_2 different alkyl groups) or ester hydrolysis ($OR_2^- = OH^-$). Under limiting conditions the rate of pathway C is simply governed by that of OR_1^- loss and is independent of $[OH^-]$.

Direct addition of the neutral alcohol has also been observed for[42] $PtCl(PPh_3)_2CO^+$ in DMF. In this case, Scheme IIIA, the addition rate is first-order in alcohol and Pt–CO concentrations while the reverse (hydrolysis) rate is first-order in the concentrations of alkoxycarbonyl and hydrogen ion. Finally, "tetrahedral intermediates", Scheme IIIB, of the type proposed for organic systems (see below) may be important in some systems.[27a] With few exceptions organic ester hydrolysis occurs via a tetrahedral intermediate resulting from nucleophilic attack on the carbonyl function as shown in Scheme IV.[43] Both acid and base (hydroxide or other nucleophile) catalyzed pathways are significant in most systems. Thus the rates are first-order in $[H^+]$ at low pH (k_{H^+}), first-order in $[OH^-]$ at higher pH (k_{OH^-}, Scheme IIIB), and pass through a minimum (where contributions from k_{H_2O}, arising from nucleophilic attack by water, are most significant) at intermediate pH (if $k_{H^+} = k_{OH^-}$, at pH 7). The dissociative mechanism (Scheme IIIC) discussed above for organometallic systems, "BAC1" or SN1 in organic parlance, is not found for purely organic systems.

The rate law determined for ester hydrolysis in the present study (eq 5) is consistent with Scheme III but is also of the form generally found for organic esters. The magnitudes of both $[H^+]$- and $[OH^-]$-dependent terms are consistent with Scheme IV, given that both acid- and base-catalyzed paths are sensitive to the steric and electronic nature of the group attached to the acyl carbon.[43-45] The magnitude of the base-hydrolysis term is 100 times smaller than that for R = *tert*-butyl and $R_1 = C_2H_5$ and 10 000 times smaller than for $R = CH_3$.[43-45] However, it is equally consistent to ascribe the $[H^+]$-dependent term in eq 6 to protonation of the alkoxy oxygen (followed by elimination of ROH, Scheme IIIA) as found in ref 42. In any event, the pH-independent term ($d = 1.6 \times 10^{-7}$ s^{-1}) is several orders of magnitude larger than expected if only Scheme IV were operative in this system. For Scheme IVb with H_2O, instead of OH^- as nucleophile, the rate constant should be[45] reduced by at least 6–8 orders of magnitude ($k < 10^{-12}$ s^{-1}). Consequently, we suggest that the pH-independent path corresponds to "ester hydrolysis" according to Scheme IIIC. Within this model, d is the rate constant for $C_2H_5O^-$ loss from the ethoxycarbonyl to yield $Co(en)_2(OH_2)(CO)^{3+}$. (The latter has only a transient existence, of course, because nucleophilic attack by OH^- and/or H_2O yields the CO_2^{2-} complex.) The very small magnitude of the rate of ethoxide loss suggests a very high affinity of $Co(en)_2(H_2O)(CO)^{3+}$ for OR^- (eq 20), probably[46] at least 7 orders of magnitude greater than that of $Ru_3(CO)_{12}$ for CH_3O^-, i.e. $K_{-20} \geq 10^{10}$ M^{-1}. This is not a surprising result given the high charge on the putative carbonyl complex and the great unlikeliness of significant back-bonding in the species.

$$Co(en)_2(H_2O)(C(O)OR)^{2+} \rightleftharpoons Co(en)_2(H_2O)(CO)^{3+} + OR^- \quad (20)$$

Scheme IV

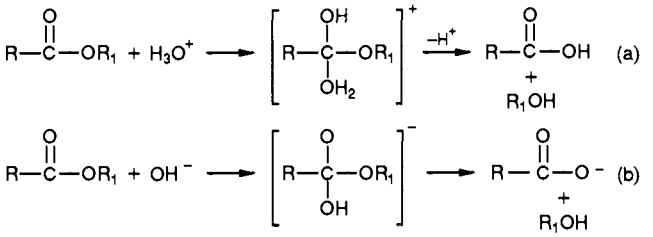

Both $Co(en)_2(OH_2)(CO_2H)^{2+}$ and $Co(en)_2(OH_2)(CO_2Et)^{2+}$ produce up to ca. 0.1 mol of CO/mole of complex in acidic solutions. In 4–12 M HCl solution, much higher yields of CO are found (Tables VIII and IX) and the major cobalt product shifts from Co(II) to Co(III). The blanks (Table VIII) establish that Co–C bond breaking to yield Co(III) and free formic acid or ethyl formate does not occur to a significant extent; if it did, Co(III) and formate (rather than Co(III) and CO) would be the major products. (Ethyl formate, if released from the Co(III), would undergo rapid hydrolysis, $k_{obsd} \geq 2 \times 10^{-2}$ s^{-1} in these media.[47]) In the HCl solutions the first-order dependence of the rate on the concentrations of the cobalt complex and HCl is consistent with eq 21–23 as the CO-forming pathway[48] (cf. Scheme IIIA). (Since

$$(Cl)Co(en)_2(C(O)OR)^+ + H^+ \rightleftharpoons (Cl)Co(en)_2(C(O)O(H)R)^{2+} \quad (21)$$

$$(Cl)Co(en)_2(C(O)O(H)R)^{2+} \rightleftharpoons (Cl)Co(en)_2(CO)^{2+} + ROH \quad (22)$$

$$(Cl)Co(en)_2(CO)^{2+} \xrightarrow{Cl^-} (Cl)_2Co(en)_2^+ + CO \quad (23)$$

it is likely that Cl^- replaces water as the trans ligand at high $[Cl^-]$, the reactants are written as chloro complexes in eq 21–23.) Equilibrium 22 is related to equilibrium 20 through the protonation constant for RO^- and the equilibrium constant for replacement of water by Cl^- and $K_{22} \simeq 10^{15}K_{20}$ is expected.[49] Thus protonation (eq 21) both suppresses CO_2 elimination (Scheme I, R = H) and

(42) Byrd, J. E.; Halpern, J. *J. Am. Chem. Soc.* **1971**, *93*, 1634.
(43) March, J. *Advanced Organic Chemistry*, 3rd ed.; Wiley: New York, 1985; pp 334–8.
(44) (a) Bilkadi, A.; de Lorimier, R.; Kirsch, J. F. *J. Am. Chem. Soc.* **1975**, *97*, 4317. (b) Halonen, E. A. *Acta Chem. Scand.* **1956**, *10*, 435. (c) Salomaa, P. *Acta Chem. Scand.* **1960**, *14*, 577. (d) Jencks, W. P.; Carriuolo, J. *J. Am. Chem. Soc.* **1961**, *83*, 1743.
(45) (a) Johnson, S. L. *Adv. Phys. Org. Chem.* **1967**, *5*, 237. (b) Kirsch, J. F.; Jencks, W. P. *J. Am. Chem. Soc.* **1964**, *86*, 837.
(46) The estimate $K_{-20} = 10^{10}$ M^{-1} assumes that the rate constant for OR^- elimination $k_{3c} \propto K$; from ref 40 and 41 it appears more likely that $k_{3c} \propto K^2$, which yields $K_{-20} = 10^{16}$ M^{-1} as estimate (since k_{-3c} must be less than or equal to diffusion controlled, ca. 10^9 M^{-1} s^{-1}).
(47) Bell, R. P.; Dowding, A. L.; Noble, J. A. *J. Chem. Soc.* **1955**, 3106.
(48) (a) As considered in Scheme IV, the –C(O)(OR) moiety is expected to protonate at the acyl carbon,[48b] thereby facilitating nucleophilic attack by water (saponification) or by an alcohol (esterification) to give a tetrahedral species. The protonated species in Schemes IIIA and IVA differ in composition by a water molecule and can, in principle, be distinguished by determining whether the rates are a function of $[H^+]$ or H_0.[48c] Although our studies are not sufficiently detailed to make such distinctions, it is not obvious how CO could result from Scheme IV while Scheme III provides a rationale for both CO formation and ester formation. (b) The pK_a of ethyl acetate (protonated at the acyl carbon) is –7: Lane, C. A. *J. Am. Chem. Soc.* **1964**, *86*, 2521. (c) See: Yates, K. *Acc. Chem. Res.* **1971**, *4*, 171.
(49) The production of CO in the pH 0–3 solutions could result from a competition of eq 24 and 25 (Scheme IIIC) with Schemes I and II, followed

$$HOCo(en)_2(C(O)OH)^+ \rightleftharpoons HOCo(en)_2(CO)^{2+} + OH^- \quad (24)$$

$$HOCo(en)_2(C(O)OH_2)^{2+} \rightleftharpoons HOCo(en)_2(CO)^{2+} + H_2O \quad (25)$$

by CO loss and reaction of the Co(III) product with $Co(en)_2CO_2$, Co(I), or Co(0). Because "OH^-" loss should be favored by protonation and by the presence of a π-donor ligand (OH^-) trans to the incipient CO, the reactants invoked in eq 24 and 25 are tautomers of the dominant forms of the complex, $Co(en)_2(H_2O)(CO_2)^+$ and $Co(en)_2(H_2O)(CO_2H)^{2+}$ (see eq 1, 2 and 1′, 2′). Alternatively, CO might be formed by an "inner-sphere" path such as eq 26.

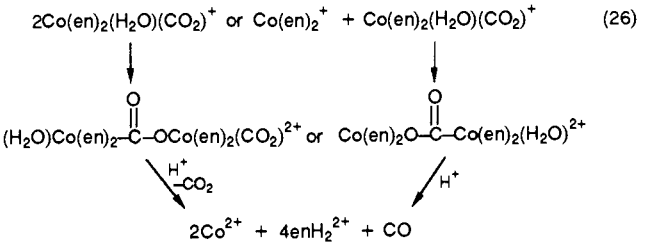

Such paths should be second order in the carboxylate complex while eq 24 and 25 would be first-order in the reactant. Since the CO formation path contributes so little to the overall decay and our concentration range is not large, we cannot rule out the inner-sphere path eq 26.

Table XI. Summary of Selected Equilibrium and Kinetic Parameters at 25 °C

Acidity	
$Co(en)_2(H_2O)(CO_2H)^{2+} \rightleftharpoons Co(en)_2(H_2O)(CO_2)^+ + H^+$	$pK_{a1} = 2.8 \pm 0.2$
$Co(en)_2(H_2O)(CO_2)^+ \rightleftharpoons Co(en)_2(OH)(CO_2) + H^+$	$pK_{a2} = 3.8 \pm 0.2$
$Co(en)_2(H_2O)(CO_2Et)^{2+} \rightleftharpoons Co(en)_2(OH)(CO_2Et)^+ + H^+$	$pK_{a3} = 8.7 \pm 0.2$
$Co(en)_2(H_2O)(CO_2)^+ \rightleftharpoons Co(en)_2(OH)(CO_2H)^+$	$K \approx 10^{-6}$
Reductive Elimination/Homolysis	
$Co(en)_2(H_2O)(CO_2H)^{2+} \rightarrow CO_2 + Co(en)_2(H)(H_2O)^{2+}$ or $\bullet CO_2H + Co(en)_2^{2+}$	$k < 10^{-5}\ s^{-1}$
$Co(en)_2(H_2O)(CO_2)^+ \rightarrow CO_2 + Co(en)_2^+$ or $\bullet CO_2^- + Co(en)_2^{2+}$	$k = 4.5 \times 10^{-3}\ s^{-1}$
$Co(en)_2(OH)(CO_2) \rightarrow CO_2 + Co(en)_2^+ + OH^-$ or $\bullet CO_2^- + Co(en)_2(OH)^+$	$k < 10^{-8}\ s^{-1}$
Heterolysis	
$Co(en)_2(H_2O)(CO_2H)^{2+} + H_3O^+ \rightarrow Co(en)_2(H_2O)_2^{3+} + HCO_2H$	$k < 10^{-5}\ M^{-1}\ s^{-1}$
$Co(en)_2(OH)(CO_2) + OH^- \xrightarrow{H_2O} Co(en)_2(OH)_2^+ + HCO_2^-$	$k < 10^{-6}\ M^{-1}\ s^{-1}$
Nucleophilic Elimination	
$Co(en)_2(H_2O)(CO_2Et)^{2+} \rightarrow EtO^- + Co(en)_2(H_2O)(CO)^{3+}$	$k \approx 10^{-7}\ s^{-1}$

promotes CO formation (eq 22).

In short, the behavior inferred for other oxy, alkoxy, and hydroxycarbonyl complexes summarized in Scheme III provides a useful framework for understanding both the hydrolysis of $Co(en)_2(OH_2)(CO_2Et)^{2+}$ and the formation of CO from $Co(en)_2(H_2O)(CO_2R)^{2+}$.

Overview. Table XI summarizes selected aspects of the reactivity of **1** and **2** in aqueous media. As noted earlier, for $Co(en)_2^{3+}$, $-C(O)OEt^-$, $-C(O)OH^-$, and $-C(O)O^{2-}$ are strong field, trans-labilizing ligands as revealed by both the structural and spectroscopic studies. Bound to $Co(en)_2^{3+}$, $-CO_2H^-$ is a fairly strong carboxylic acid, and, in water, the hydroxycarbonyl is present only below about pH 3.

On the basis of our current knowledge,[50] it is very likely that $Co(en)_2(H_2O)(CO_2H)^{2+}$ is formed via the addition[51] of CO_2^- to $Co(en)_2^{2+}$, with the latter "radicals" being generated in the UV photolysis of the $Co(en)_2(C_2O_4)^+$: The UV excitation leads effectively to a ligand-to-metal charge-transfer state of the cobalt complex, i.e. $Co^{II}(en)_2(C_2O_4^-)^+$. As is generally found, the radical RCO_2 (i.e., $C_2O_4^-$) undergoes rapid decarboxylation to produce $R^\bullet$ (i.e., CO_2^-). The rapid addition of $R^\bullet$ to the highly labile Co(II) center is relatively common. Unfortunately, it is not clear to what extent homolysis[52] of the $CoCO_2$ species (to $Co^{II} + CO_2^-$) competes with reductive elimination of carbon dioxide to yield Co(I) in the decomposition of the complexes. However, neither "acidolysis" (attack of H^+ on the Co–C bond)[52] nor base hydrolysis of the cobalt(III) amine moiety[53] to give free formate (or ethyl formate) is detected in this system. Furthermore, except in concentrated HCl solutions, the reductive elimination process dominates markedly over nucleophilic elimination to yield the Co(III)–CO complex. Indeed our results suggest that nucleophilic elimination is quite unfavorable thermodynamically and that the affinity of $Co(en)_2(H_2O)(CO)^{3+}$ for nucleophiles such as OH^- and $C_2H_5O^-$ is very large. While this result is not unexpected (at least in a qualitative sense), its implications for CO_2 reduction chemistry may not have been widely appreciated. In these cationic complexes, CO formation is intrinsically suppressed. Such complexes may thus afford the opportunity for template hydrogenation of bound CO_2 (deprotonated formate, CO_2^{2-}) to bound dihydroxymethyl/$-CH(OH)_2$ or $-CH(O)$. This possibility and further characterization of the remarkably unreactive $Co(en)_2(OH)(CO_2)$ are the focus of ongoing studies.

Acknowledgment. A fellowship awarded to N.E.K. by the "Consejo Nacional de Investigaciones Cientificas y Tēcnicas de la Republica Argentina" is gratefully acknowledged. We thank E. Fujita for running the NMR spectra, M. Andrews, D. Cabelli, and E. Norton for guidance in developing the analytical procedures, and M. Andrews, M. Bullock, H. A. Schwarz, and S. Seltzer for helpful comments. This research was carried out at Brookhaven National Laboratory under Contract DE-AC02-76CH00016 with the U.S. Department of Energy and supported by its Division of Chemical Sciences, Office of Basic Energy Sciences.

Registry No. 1, 121596-42-7; **2**, 121596-44-9; $[(en)_2Co(C_2O_4)]Cl$, 17439-00-8; $enH_2(CF_3CO_2)_2$, 121575-05-1; $[Co(en)_2(OH_2)(CO_2C_2H_5)](PF_6)_2$, 121596-46-1; $Co(en)_2(CH_3CN)(CO_2Et)^{2+}$, 121596-47-2; $Co(en)_2(OH)(CO_2Et)^+$, 121596-48-3; $Co(en)_2(OH)(CO_2)$, 121596-49-4.

Supplementary Material Available: Tables of final thermal parameters, calculated hydrogen atom positions, and intraanion bond distances and angles (6 pages); table of observed and calculated structure factors (8 pages). Ordering information is given on any current masthead page.

(50) (a) Some of the observations reported in ref 6 remain unexplained,[50b] for example, the nature of the "short-lived" (SL) intermediate observed in the flash-photolysis work. Since its decay is accompanied by the formation of little Co_{aq}^{2+}, it may be that SL is the cis isomer of $Co(en)_2(H_2O)(CO_2H)^{2+}$ and that cis to trans isomerization is being monitored on the $1-10^{-3}$-s time scale. (b) There are significant contrasts in the behavior of the $Co(en)_2^-$ and $Co(NH_3)_4^-$ complexes: the ammine-based analogues display O_2-dependent quantum yields at low pH[6] and yield Co(II) (not Co(III)) in concentrated HCl solutions.[50c] Possibly the species active in the tetraammine system is actually a lower ammine (e.g., $Co(NH_3)_3$) species, and this is the origin of the reactivity difference. (c) Way, H.; Filipescu, N. *Inorg. Chem.* **1969**, *8*, 1609.

(51) Addition of $^\bullet CO_2^-$ to substitution-labile metal centers is a rather general reaction. (a) See: Goldstein, S.; Czapski, G.; Cohen, H.; Meyerstein, D. *J. Am. Chem. Soc.* **1988**, *110*, 3903 and references cited therein. (b) For addition of CO_2^- to Co(II) centers, see ref 20b and 28. (c) For addition of other radicals to Co(II), see e.g. ref 18.

(52) Espenson, J. H. *Adv. Inorg. Bioinorg. Mech.* **1982**, *1*, 1 and references therein.

(53) Tobe, M. L. *Adv. Inorg. Bioinorg. Mech.* **1983**, *2*, 1 and references therein.